ARTICLE

TRAF2 regulates T cell immunity by maintaining a Tpl2-ERK survival signaling axis in effector and memory CD8 T cells

Xiaoping Xie[1], Lele Zhu[1], Zuliang Jie[1], Yanchuan Li[1], Meidi Gu[1], Xiaofei Zhou[1], Hui Wang[1,2], Jae-Hoon Chang[1,3], Chun-Jung Ko[1], Xuhong Cheng[1] and Shao-Cong Sun[1,4]

Generation and maintenance of antigen-specific effector and memory T cells are central events in immune responses against infections. We show that TNF receptor-associated factor 2 (TRAF2) maintains a survival signaling axis in effector and memory CD8 T cells required for immune responses against infections. This signaling axis involves activation of Tpl2 and its downstream kinase ERK by NF-κB-inducing kinase (NIK) and degradation of the proapoptotic factor Bim. NIK mediates Tpl2 activation by stimulating the phosphorylation and degradation of the Tpl2 inhibitor p105. Interestingly, while NIK is required for Tpl2-ERK signaling under normal conditions, uncontrolled NIK activation due to loss of its negative regulator, TRAF2, causes constitutive degradation of p105 and Tpl2, leading to severe defects in ERK activation and effector/memory CD8 T cell survival. Thus, TRAF2 controls a previously unappreciated signaling axis mediating effector/memory CD8 T cell survival and protective immunity.

Keywords: T cell survival; Effector and memory CD8 T cells; Protective immunity; Bacterial infection; TRAF2; NIK; Tpl2

Cellular & Molecular Immunology (2021) 18:2262–2274; https://doi.org/10.1038/s41423-020-00583-7

INTRODUCTION

CD8 T cells play a crucial role in immune responses against intracellular pathogens, such as bacteria and viruses, as well as cancer.[1,2] Upon activation by antigens, CD8 T cells undergo clonal expansion and differentiation, generating a large number of effector T cells that participate in pathogen clearance.[3] Primary immune responses also lead to the generation of long-lived memory T cells that provide long-term protective immunity against reinfection with the same pathogens.[3] The Bcl2 family of proteins plays an important role in regulating the fate of immune cells, with the survival and death of T cells being critically influenced by the balance between antiapoptotic and proapoptotic Bcl2 family members.[4,5] In particular, the proapoptotic member Bim has been shown to mediate the apoptosis of activated T cells and limit T cell memory.[6–8] T cell activation is associated with phosphorylation-dependent Bim degradation, constituting a mechanism to promote T cell survival.[9–11] The MAP kinase (MAPK) ERK is involved in Bim degradation induced by the T cell receptor (TCR) and the costimulatory receptor CD28; however, the signaling axis linking the TCR/CD28 signals to ERK activation in effector and memory T cells is obscure.

Tumor necrosis factor receptor (TNFR)-associated factors (TRAFs) are a family of structurally related proteins known to function as adapters mediating signal transduction from TNFR superfamily members in innate immunity and inflammation.[12–14] A recent study revealed that genetic deficiency in one TRAF family member, TRAF2, perturbs CD8 T cell homeostasis, although the role of TRAF2 in antigen-specific CD8 T cell responses and immunological memory has not been defined.[15] In addition, the mechanism by which TRAF2 regulates T cell signaling is unclear. It has been suggested that TRAF2 regulates sensitivity to IL-15; however, TRAF2 deficiency does not inhibit IL-15-stimulated signaling events, including activation of AKT and STAT5.[15] Based on studies in other cell types, the function of TRAF2 appears to be complex; it can function as a signaling adapter, a lysine 63 (K63)-specific E3 ubiquitin ligase, or a component of a K48-specific E3 ubiquitin ligase complex: cIAP-TRAF2-TRAF3.[14,16] A well-defined target of the cIAP-TRAF2-TRAF3 E3 complex is NF-κB-inducing kinase (NIK), a central component of the noncanonical NF-κB pathway.[17] We have previously shown that NIK is dispensable for naïve T cell activation but is required for recall responses.[18]

In the present study, we demonstrate that TRAF2 facilitates effector and memory CD8 T cell responses by regulating NIK and through a downstream survival signaling axis involving the MAPK kinase kinase (MAP3K) Tpl2 and the MAPK ERK. Tpl2 is known as an innate immune kinase that complexes with the NF-κB1 precursor protein p105, which functions as both an inhibitor and stabilizer of Tpl2.[19–21] Innate immune stimuli induce IκB kinase (IKK)-mediated phosphorylation and degradation of p105, causing the activation and subsequent degradation of Tpl2.[22,23] Our present study demonstrates that in effector and memory CD8 T cells, NIK mediates TCR/CD28-stimulated IKK activation and p105 phosphorylation, thereby facilitating activation of the Tpl2-ERK signaling axis. Interestingly, TRAF2 deficiency causes aberrant NIK accumulation and constitutive degradation of p105 and Tpl2, leading to a severe defect in ERK activation and memory CD8 T cell survival. These results suggest that TRAF2 mediates the

[1]Department of Immunology, The University of Texas MD Anderson Cancer Center, 7455 Fannin Street, Box 902, Houston, TX 77030, USA; [2]Jiangsu Key Laboratory of Immunity and Metabolism, Department of Pathogenic Biology and Immunology, Xuzhou Medical University, 209 Tongshan Road, Xuzhou 221004 Jiangsu, China; [3]College of Pharmacy, Yeungnam University, Gyeongsan 712-749, Republic of Korea and [4]MD Anderson Cancer Center UT Health Graduate School of Biomedical Sciences, Houston, TX 77030, USA
Correspondence: Shao-Cong Sun (ssun@mdanderson.org)

Received: 25 June 2020 Accepted: 21 October 2020
Published online: 17 November 2020

© CSI and USTC 2020

survival of effector and memory CD8 T cells by maintaining the Tpl2-ERK signaling axis.

RESULTS

TRAF2 is crucial for CD8 T cell responses to bacterial infections

To study the role of TRAF2 in regulating T cell functions, we generated T cell-conditional *Traf2* knockout (*Traf2*-TKO) mice (Supplementary Fig. 1a, b). Consistent with a previous study,[15] *Traf2*-TKO mice had perturbed T cell homeostasis, characterized by a reduced frequency and absolute number of memory-like ($CD44^{hi}$) CD8 but not CD4 T cells (Supplementary Fig. 1c, d). Interestingly, however, this phenotype was no longer detected when *Traf2*-TKO mice were crossed with OT-I TCR-transgenic mice (Supplementary Fig. 1e). OT-I mice produced CD8 T cells with a recombinant TCR responding to a chicken ovalbumin (OVA) epitope, $OVA_{257–264}$, but not to commensal antigens.[24,25] These results suggested that TRAF2 might not be important for naïve CD8 T cell responses to homeostatic cytokines. Indeed, *Traf2*-TKO OT-I CD8 T cells displayed normal proliferation and signaling when stimulated with the homeostatic cytokines IL-2, IL-7, or IL-15 (Supplementary Fig. 2a, b). The same result was obtained even when the cells were stimulated with higher doses of IL-15 (Supplementary Fig. 2c). On the other hand, TRAF2-deficient memory OT-I CD8 T cells exhibited a partial defect in IL-15-induced proliferation despite normal IL-15 signaling (Supplementary Fig. 2d, e). Notably, TRAF2 deficiency also partially inhibited the proliferation of memory but not naïve OT-I CD8 T cells stimulated with anti-TCR and anti-CD28 agonistic antibodies (Supplementary Fig. 2f, g). These results suggest that TRAF2 may regulate CD8 T cell responses to both IL-15 and antigens.

To examine the role of TRAF2 in mediating antigen-specific CD8 T cell responses in vivo, we employed a bacterial infection model using a recombinant *Listeria monocytogenes* (LM) strain expressing chicken ovalbumin (LM-OVA).[26] LM is an intracellular bacterial pathogen that induces strong CD8 T cell responses, which are required for controlling LM infection and providing protective immunity.[27,28] During a primary immune response, antigen-specific effector T cells undergo an initial expansion phase, which typically peaks around day 7, followed by a contraction phase, leaving a small percentage to form long-lived memory CD8 T cells.[29–32] To evaluate primary immune responses, we analyzed the T cells after 7 days of LM-OVA infection. Compared to wild-type mice, *Traf2*-TKO mice had a significantly lower frequency and absolute number of splenic CD8 T cells, although the frequency and absolute number of CD4 T cells were comparable between wild-type and *Traf2*-TKO mice (Fig. 1a). TRAF2 deficiency caused a specific reduction in the frequency of $CD44^{hi}$ CD8 T cells, representing effector T cells, whereas the frequency of $CD44^{lo}$ naïve CD8 T cells was concomitantly increased in *Traf2*-TKO mice (Fig. 1b). Consistent with these results, *Traf2*-TKO mice exhibited a drastically reduced frequency of antigen (OVA)-specific IFN-γ-producing splenic CD8 effector cells (Fig. 1c). The frequency of CD4 effector T cells responding to the Listeria antigen $LLO_{190–204}$ was also reduced, albeit less profoundly than that of the abovementioned CD8 effector cells (Fig. 1d). In line with their reduced frequency of CD8 effector T cells, *Traf2*-TKO mice had a significantly higher LM burden in the spleen and liver than did wild-type control mice (Fig. 1e). To ensure that the results obtained with *Traf2*-TKO mice were not due to abnormal T cell homeostasis, we repeated the LM-OVA infection experiment using *Traf2*-TKO OT-I mice, which had normal T cell homeostasis (Supplementary Fig. 1e). As seen with *Traf2*-TKO mice, *Traf2*-TKO OT-I mice had impaired CD8 T cell responses to LM-OVA infection (Fig. 1f), confirming a crucial role for TRAF2 in regulating antigen-specific CD8 T cell responses. In addition, these results suggest a role for TRAF2 in regulating the generation or maintenance of antigen-specific effector T cells.

TRAF2 is required for memory CD8 T cell responses and protective immunity

To examine the role of TRAF2 in regulating memory T cell responses, we infected *Traf2*-TKO and wild-type control mice with LM-OVA for 60 days and then reinfected the mice for 3 days to trigger memory responses (Fig. 2a). Compared to the primary response (Fig. 1c, d), the memory response generated a much higher frequency of antigen-specific CD8 effector T cells (Fig. 2b, c). Importantly, as seen with the primary immune response, *Traf2*-TKO mice exhibited a drastic reduction in the frequency of $OVA_{257–264}$-specific effector CD8 T cells and, to a lesser extent, $LLO_{190–204}$-specific effector CD4 T cells in the memory response, coupled with a significantly higher Listeria count in the liver and spleen (Fig. 2b–d).

To further confirm the role of TRAF2 in regulating memory CD8 T cell responses, we employed a T cell adoptive transfer model. We transferred the same number of wild-type or TRAF2-deficient memory OT-I CD8 T cells into B6.SJL mice and then infected the recipient mice with LM-OVA (Fig. 2e). Compared to recipients of TRAF2-deficient memory OT-I CD8 T cells, recipients of wild-type memory OT-I CD8 T cells displayed a much more robust memory response, as revealed by serum IFN-γ measurements 4 h after LM-OVA infection (Fig. 2f). Twenty-four hours after LM-OVA infection, recipient mice had a much lower frequency and absolute number of *Traf2*-TKO OT-I T cells than of wild-type OT-I T cells (Fig. 2g). In addition, the population of *Traf2*-TKO OT-I T cells also contained a lower frequency and absolute number of $OVA_{257–264}$-specific IFN-γ-producing effector T cells than of wild-type OT-I T cells (Fig. 2h). Consistent with these findings, *Traf2*-TKO OT-I recipient mice had a higher Listeria load in the spleen and liver than did wild-type OT-I recipient mice (Fig. 2i). These results further confirm the role of TRAF2 in mediating memory CD8 T cell responses to bacterial infections.

The important role of TRAF2 in mediating CD8 memory T cell responses prompted us to examine the effect of TRAF2 deficiency on protective immunity. Wild-type and *Traf2*-TKO mice were infected with a sublethal dose of LM-OVA, and after 30 days, the mice were reinfected with a lethal dose of LM-OVA (Fig. 2j). While wild-type mice were largely protected from LM-OVA reinfection, a high percentage of *Traf2*-TKO mice succumbed to reinfection (Fig. 2k). We also employed a cancer vaccine model involving vaccination of wild-type and *Traf2*-TKO mice with LM-OVA and subsequent challenge with syngeneic B16 melanoma cells expressing OVA (B16-OVA) (Fig. 2l). Compared to wild-type mice, *Traf2*-TKO mice exhibited a profoundly increased tumor growth rate and decreased survival rate, suggesting that TRAF2 deficiency impaired protective immunity (Fig. 2m, n). These results suggest an indispensable role for TRAF2 in mediating memory CD8 T cell responses and protective immunity.

TRAF2 mediates the survival of effector and memory CD8 T cells

The results presented above suggested a crucial role for TRAF2 in regulating the generation or maintenance of effector and memory CD8 T cells. While this function of TRAF2 might involve regulation of CD8 T cell expansion, as suggested by the results of in vitro studies (Supplementary Fig. 2d, g), we also examined the role of TRAF2 in regulating the survival of effector and memory CD8 T cells. Remarkably, 7 days after LM-OVA infection, *Traf2*-TKO mice had a significantly higher frequency of apoptotic CD8 T cells than wild-type mice, as determined based on staining with Annexin V and propidium iodide (PI) (Fig. 3a). This phenotype was specific for effector ($CD44^{hi}$) CD8 T cells, since the frequency of apoptotic naïve ($CD44^{lo}$) CD8 T cells was comparable between wild-type and *Traf2*-TKO mice (Fig. 3b). These results were in line with the selective reduction in effector CD8 T cells in LM-OVA-infected *Traf2*-TKO mice (Fig. 1b).

To examine the role of TRAF2 in regulating the survival of memory CD8 T cells, we infected wild-type and *Traf2*-TKO mice

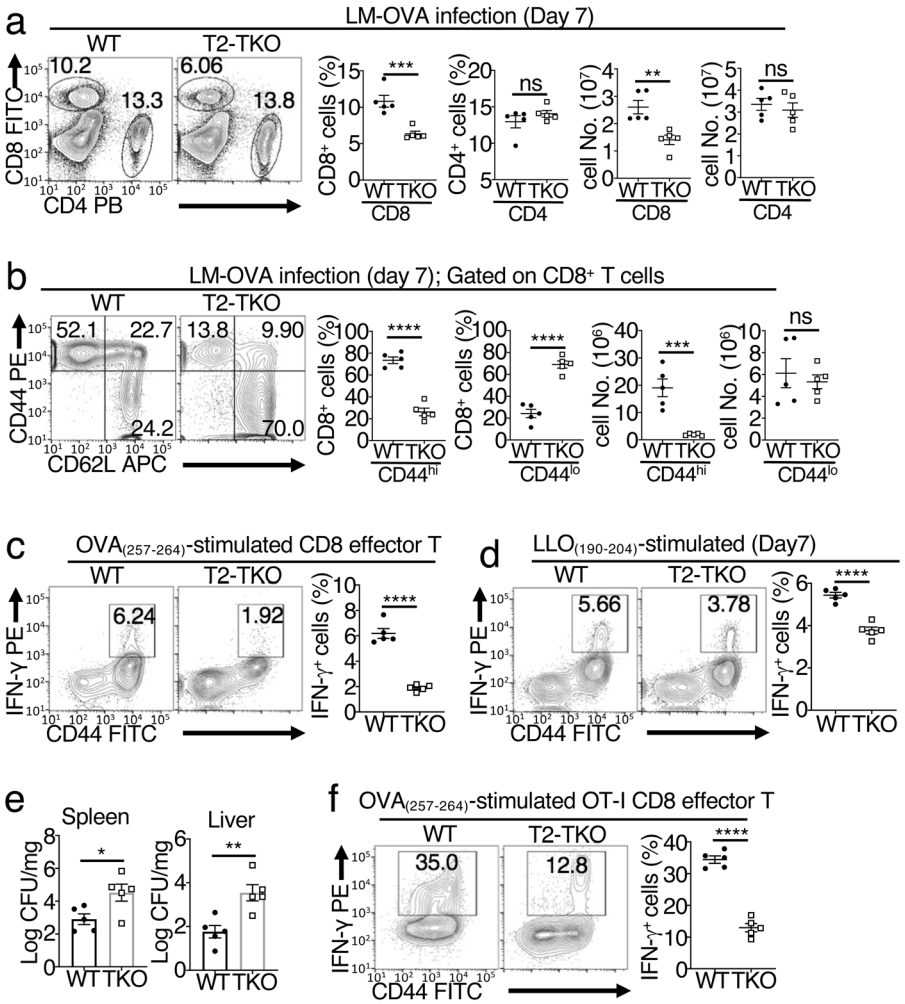

Fig. 1 TRAF2 deficiency dampens antibacterial immune responses. **a**–**d** Measuring primary T cell responses 7 days after infection of wild-type (WT) and *Traf2*-TKO mice with LM-OVA ($n = 5$). Flow cytometric analysis of the percentages and absolute numbers of splenic CD4 and CD8 T cells (**a**) or naïve ($CD44^{lo}$) and memory ($CD44^{hi}$) CD8 T cells (**b**). ICS and flow cytometric analysis of IFN-γ-producing CD8 (**c**) and CD4 (**d**) T cells in splenocytes restimulated in vitro for 6 h with $OVA_{257–264}$ (**c**) or $LLO_{190–201}$ (**d**) peptide in the presence of monensin. **e** Bacterial load in the spleen and liver in wild-type and *Traf2*-TKO mice 5 days after infection with LM-OVA ($n = 5$). **f** Flow cytometric analysis of IFN-γ-producing CD8 T cells in the spleens of wild-type and *Traf2*-TKO OT-I mice 7 days after infection with LM-OVA ($n = 5$). Data are representative of three independent experiments. Summary data are shown as the mean ± SEM values, and *p* values were determined by unpaired Student's *t* test. $^*p < 0.05$; $^{**}p < 0.01$; $^{***}p < 0.001$; $^{****}p < 0.0001$; ns not significant

with LM-OVA for 60 days. Sixty days after LM-OVA infection, *Traf2*-TKO mice had a profound reduction in the frequency and absolute number of CD8 T cells (Fig. 3c). The frequency of CD4 T cells was also reduced in *Traf2*-TKO mice, but the absolute number of CD4 T cells was not significantly different between wild-type and *Traf2*-TKO mice (Fig. 3c). The loss of CD8 T cells in the *Traf2*-TKO mice was specific for $CD44^{hi}$ memory CD8 T cells, since wild-type and *Traf2*-TKO mice did not have significant differences in the absolute number of CD8 naïve T cells (Fig. 3d). Consistent with these findings, compared to wild-type mice, *Traf2*-TKO mice exhibited a much higher level of apoptosis in the memory ($CD44^{hi}$) but not the naïve ($CD44^{lo}$) CD8 T cell population (Fig. 3e, f). We also examined CD8 T cell apoptosis during recall responses following rechallenge of the infected mice with LM-OVA (Supplementary Fig. 3a). LM-OVA reinfection induced a much lower frequency of $CD44^{hi}$ antigen-specific CD8 effector T cells in *Traf2*-TKO mice than in wild-type mice, as determined based on staining with OVA peptide-loaded MHCI tetramers (Fig. 3g). Furthermore, more than 70% of the antigen-specific ($tetramer^+$) CD8 T cells in the spleen of *Traf2*-TKO mice were apoptotic, a much higher percentage than that in wild-type mice (Fig. 3h). *Traf2*-TKO mice also exhibited an increased frequency of apoptosis within the $tetramer^-$ CD8 T cell population, albeit a less profound increase than in the $tetramer^+$ population, likely due to the presence of memory CD8 T cells specific for other LM epitopes (Fig. 3i). Indeed, when gated based on the memory T cell marker CD44, *Traf2*-TKO mice did not show increased apoptosis within the naïve ($CD44^{lo}$) CD8 T cell population (Supplementary Fig. 3a, b).

We next examined whether the homeostatic loss of memory-like CD8 T cells in *Traf2*-TKO mice (Supplementary Fig. 1c and ref. [15]) might also be due to impaired survival. Compared with wild-type control mice, *Traf2*-TKO mice had a significantly higher frequency of apoptotic cells within the $CD44^{hi}$ memory-like but not the $CD44^{lo}$ naïve CD8 T cell population (Supplementary Fig. 3c). In contrast, TRAF2 deficiency did not affect the survival of memory-like or naïve CD4 T cells, consistent with the dispensable role of TRAF2 in regulating CD4 T cell homeostasis (Supplementary Fig. 3d). Furthermore, TRAF2 deficiency had no effect on the apoptosis of OT-I CD8 T cells under homeostatic conditions (Supplementary Fig. 3e), consistent with their predominant naïve phenotype (Supplementary Fig. 1e). To further determine whether TRAF2 selectively regulates the survival of effector and memory

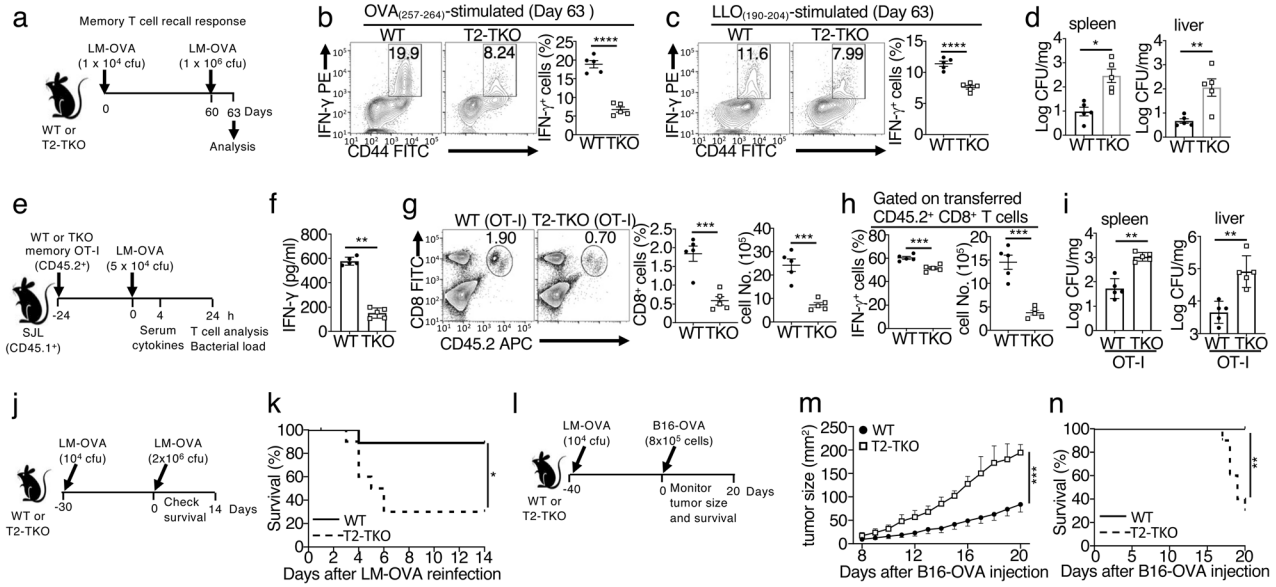

Fig. 2 TRAF2 deficiency impairs memory CD8 T cell responses and protective immunity. **a** Schematic of the experimental design, in which wild-type (WT) and *Traf2*-TKO (T2-TKO) mice were intravenously infected with a low dose (5×10^4 cfu/mouse) of LM-OVA, reinfected on day 60 with a higher dose (1×10^6 cfu/mouse) of LM-OVA, and analyzed after 3 days ($n = 5$). ICS and flow cytometric analyses of IFN-γ-producing CD8 (**b**) and CD4 (**c**) T cells among splenocytes after in vitro restimulation with the indicated peptides; analysis of the bacterial load in the spleen and liver (**d**) in the LM-OVA-infected mice described in **a**. **e**–**i** Study of memory CD8 T cell responses by adoptive transfer of wild-type or *Traf2*-TKO memory OT-I CD8 T cells (CD45.2$^+$, 5×10^5) into wild-type WT B6.SJL (CD45.1$^+$) mice prior to LM-OVA infection ($n = 5$). Schematic of the experimental design (**e**), ELISA of serum IFN-γ 4 h after infection (**f**), flow cytometric analysis of donor (CD45.2$^+$) splenic OT-I CD8 T cells (**g**) or IFN-γ-producing OT-I CD8 T cells (**h**) 24 h after infection, and bacterial load 24 h after infection (**i**). Schematic of the experimental design (**j**) and survival curves (**k**) of WT and *Traf2*-TKO mice infected with a low dose (1×10^4 cfu/mice) of LM-OVA 30 days before rechallenge with a lethal dose (2×10^6 cfu/mice) of LM-OVA ($n = 10$, $p = 0.0133$ by the log-rank test). Schematic of the experimental design (**l**), tumor size data (**m**), and survival curves (**n**) of WT and *Traf2*-TKO mice infected with a low dose (1×10^4 cfu/mice) of LM-OVA 40 days before injection (s.c.) with B16-OVA melanoma cells (8×10^5 cells/mouse) ($n = 10$). Data are representative of two (**e**–**n**) or three (**a**–**d**) independent experiments. Summary data are shown as the mean ± SEM values, and *p* values were determined by unpaired Student's *t* test (**a**–**f**, **b**–**d**, **f**–**i**), two-way ANOVA with the Bonferroni correction (**m**), or log-rank test (**k**, **n**). *$p < 0.05$; **$p < 0.01$; ***$p < 0.001$; ****$p < 0.0001$

CD8 T cells, we analyzed the apoptosis of in vitro-generated effector and memory OT-I CD8 T cells. Compared to naïve OT-I CD8 T cells, these effector and memory OT-I CD8 T cells displayed a substantially higher level of apoptosis (Fig. 3j, k). Moreover, TRAF2 deficiency greatly promoted apoptosis in effector and memory but not the naïve CD8 T cells (Fig. 3j, k). Together, these results suggest that TRAF2 regulates the survival of effector and memory but not naïve CD8 T cells.

We next examined the cell-intrinsic survival role of TRAF2 during Listeria infection using a mixed T cell transfer approach. We adoptively transferred a mixture of wild-type (CD45.1$^+$CD45.2$^+$) and *Traf2*-TKO (CD45.1$^-$CD45.2$^+$) naïve OT-I CD8 T cells into B6.SJL (CD45.1$^+$CD45.2$^-$) mice and infected the recipient mice with LM-OVA for 7 and 30 days to analyze the survival of effector and memory CD8 T cells, respectively (Fig. 3l). While the frequencies of the transferred wild-type and *Traf2*-TKO OT-I cells were initially (day 1) similar, the frequency of *Traf2*-TKO OT-I cells was drastically reduced relative to that of the wild-type OT-I cells 7 and 30 days after LM-OVA infection (Fig. 3m). Consistent with this finding, *Traf2*-TKO OT-I T cells exhibited a much higher level of apoptosis than wild-type OT-I T cells on days 7 and 30 after LM-OVA infection (Fig. 3n). These results emphasize the cell-intrinsic role of TRAF2 in mediating the survival of effector and memory CD8 T cells.

TRAF2 controls the fate of Bim in effector and memory CD8 T cells
The Bcl2 family of proteins plays a central role in regulating the apoptosis of T cells.[6,33] To examine the potential role of TRAF2 in regulating the expression of Bcl2 family members, we performed qRT-PCR analyses using in vitro-generated effector and memory CD8 T cells or naïve CD8 T cells derived from wild-type or *Traf2*-TKO mice. These analyses revealed that wild-type and *Traf2*-TKO naïve, effector, or memory CD8 T cells did not have significant differences in the mRNA expression levels of several Bcl2 family members, including the antiapoptotic members Bcl2, Bcl-Xl, Mcl1 and the proapoptotic members Bim, Bax, and Bak1 (Fig. 4a). Immunoblot assays further showed that wild-type and TRAF2-deficient CD8 T cells did not show appreciable differences in Bcl2 and Bcl-XL expression at the protein level (Fig. 4b). Interestingly, however, TRAF2 deficiency had a drastic effect on the fate of the proapoptotic protein Bim. Bim is known to be downregulated via degradation in response to TCR/CD28 stimulation, which is a crucial mechanism mediating T cell survival.[34] As expected, TCR/CD28 stimulation led to downregulation of Bim in both naïve and memory CD8 T cells (Fig. 4b). Importantly, while TRAF2 deficiency had no effect on Bim downregulation in naïve CD8 T cells, it largely blocked Bim downregulation in memory CD8 T cells (Fig. 4b). Moreover, the steady-state level of Bim was also substantially enhanced in TRAF2-deficient memory CD8 T cells, as shown by both immunoblot and flow cytometric analyses (Fig. 4b, c). We also examined Bim expression in naïve and effector T cells isolated from LM-OVA-infected mice. Once again, *Traf2*-TKO CD8 T cells exhibited a higher level of Bim expression than did wild-type CD8 T cells within the effector (CD44^{hi}) but not the naïve (CD44^{lo}) population (Fig. 4d).

To examine the functional significance of TRAF2-mediated Bim regulation, we crossed *Traf2*-TKO mice with Bim KO mice to generate double KO mice (Fig. 4e). Bim KO mice had only a slightly higher frequency of memory-like CD8 T cells than wild-type mice (Fig. 4f). Importantly, deletion of Bim significantly although not completely restored the frequency of memory-like CD8 T cells and concomitantly reduced the frequency of naïve CD8 T cells in

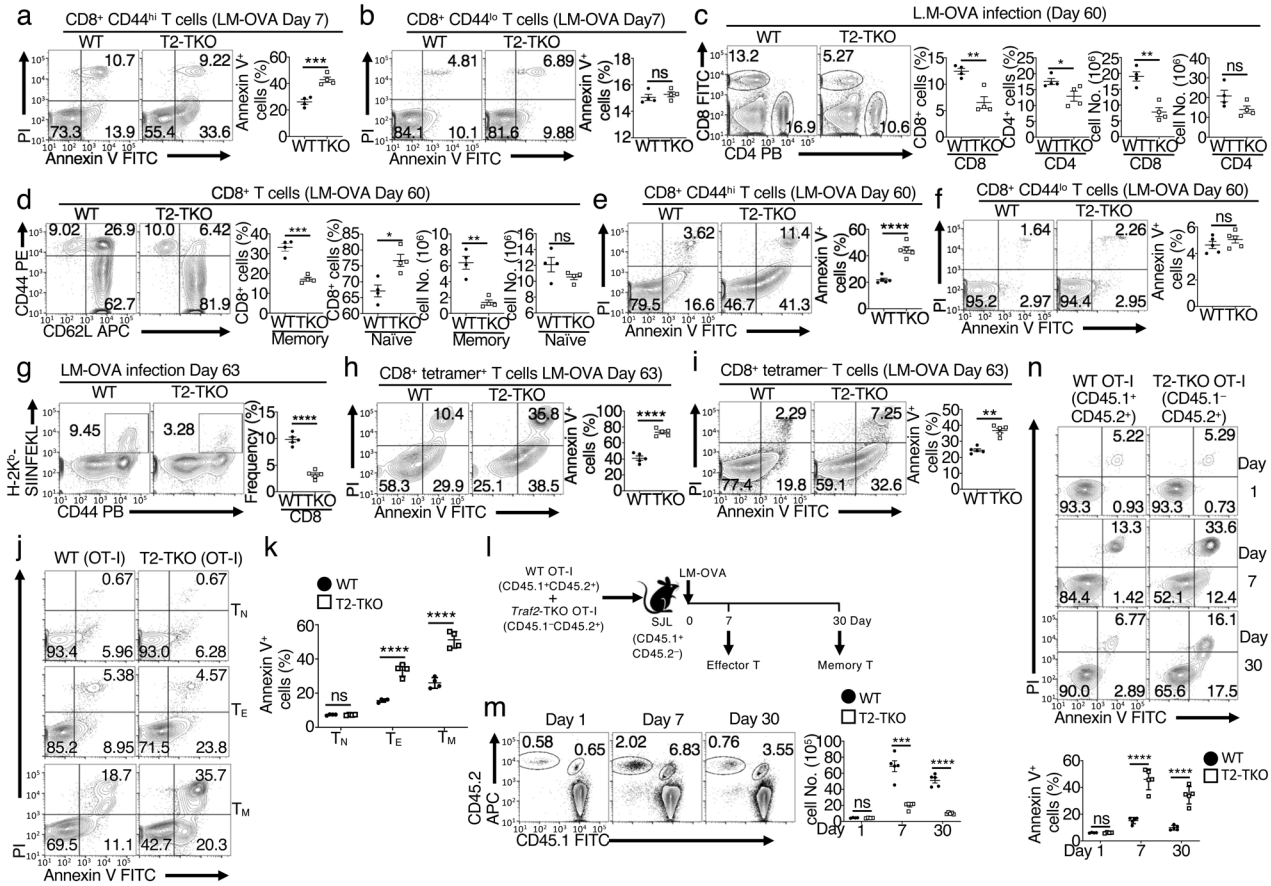

Fig. 3 TRAF2 is required for the survival of effector and memory but not naïve CD8 T cells. **a**, **b** Flow cytometric analysis of apoptotic memory ($CD44^{hi}$) and naïve ($CD44^{lo}$) CD8 T cells in the spleens of wild-type (WT) and *Traf2*-TKO mice 7 days after infection with LM-OVA ($n = 5$). Flow cytometric analysis of the percentages and absolute numbers of CD4 and CD8 T cells (**c**), the percentages and absolute numbers of naïve ($CD44^{lo}$) and memory ($CD44^{hi}$) CD8 T cells (**d**), and the percentages of apoptotic memory ($CD44^{hi}$, **e**), and naïve ($CD44^{lo}$, **f**) CD8 T cells in the spleens of WT and *Traf2*-TKO mice 60 days after infection with LM-OVA ($n = 5$). Detection of memory responses to LM-OVA infection. Flow cytometric analysis of antigen-specific CD8 T cells using the H-$2K^b$ OVA (SIINFKL) tetramer (**g**); flow cytometric analysis of apoptosis within the OVA tetramer-positive (**h**), and negative (**i**) CD8 T cell populations in the spleens of WT and *Traf2*-TKO mice infected with LM-OVA for 60 days and reinfected with LM-OVA for 3 additional days ($n = 5$). **j**, **k** Flow cytometric analysis of the percentage of apoptotic cells among naïve (T_N) or in vitro-differentiated effector (T_E), and memory (T_M) WT and *Traf2*-TKO OT-I CD8 T cells ($n = 4$), based on annexin V and PI staining. Data are presented as a representative plot (**j**) and summary graph based on multiple mice (**k**). **l**–**n** Mixed T cell transfer to study the cell-intrinsic function of TRAF2 in regulating CD8 T cell survival. **l** Schematic of the experimental design. WT B6.SJL ($CD45.1^+$, $CD45.2^-$) mice were adoptively transferred with a mixture of WT ($CD45.1^+$, $CD45.2^+$) and *Traf2*-TKO ($CD45.1^-$, $CD45.2^+$) naïve OT-I T cells (1×10^6 each). After 24 h, recipient mice were infected with 5×10^4 cfu of LM-OVA, and flow cytometric analysis of the donor T cells in the spleen at the indicated time points was performed. **m** Flow cytometric analysis of the percentages and absolute numbers of adoptively transferred WT ($CD45.1^+$, $CD45.2^+$) and *Traf2*-TKO ($CD45.1^-$, $CD45.2^+$) OT-I CD8 T cells ($n = 5$). **n** Flow cytometric analysis of the apoptosis rate of adoptively transferred WT or *Traf2*-TKO T cells ($n = 5$). Data are representative of two (**l**–**n**) or three (**a**–**k**) independent experiments. Summary data are presented as the mean ± SEM values based on multiple animals (each symbol represents a mouse). *p* values were determined by unpaired Student's *t* test. *$p < 0.05$; **$p < 0.01$; ***$p < 0.001$; ****$p < 0.0001$; ns not significant

Traf2-TKO mice (Fig. 4f). Parallel apoptosis analysis revealed that Bim deletion also prevented the aberrant apoptosis of *Traf2*-TKO memory-like CD8 T cells (Fig. 4g). Using the LM-OVA infection model, we further demonstrated that Bim deletion inhibited the apoptosis of antigen-stimulated effector and memory CD8 T cells (Fig. 4h). These results suggest that Bim regulation is one of the major mechanisms by which TRAF2 mediates effector/memory CD8 T cell survival.

TRAF2 is required for ERK activation in effector and memory CD8 T cells

To understand how TRAF2 regulates Bim expression and CD8 T cell survival, we examined the effect of TRAF2 deficiency on TCR/CD28-stimulated signaling events. TRAF2 deficiency in naïve CD8 T cells did not substantially alter the major signaling events stimulated by anti-CD3 plus anti-CD28 antibodies, including phosphorylation of TCR-proximal protein tyrosine kinases (Lck and Zap70), AKT, and MAPKs (ERK, JNK, p38) (Fig. 5a). Interestingly, TRAF2 deficiency in memory CD8 T cells attenuated TCR/CD28-stimulated phosphorylation of ERK and its upstream kinase Mek, although it did not substantially alter the phosphorylation of the other signaling factors analyzed (Fig. 5b). Immunoblot analyses using freshly prepared CD8 T cells also revealed impairment of ERK phosphorylation to the baseline level in effector and memory CD8 T cells (Fig. 5c).

To further confirm the role of TRAF2 in regulating ERK activation, we analyzed the effect of TRAF2 deficiency on ERK phosphorylation in vivo by flow cytometry. Although TRAF2 deficiency had no effect on ERK phosphorylation in naïve ($CD44^{lo}$) CD8 T cells, it significantly reduced ERK phosphorylation in memory-like ($CD44^{hi}$) CD8 T cells (Fig. 5d). Similar results were obtained in CD8 T cells derived from LM-OVA-infected mice,

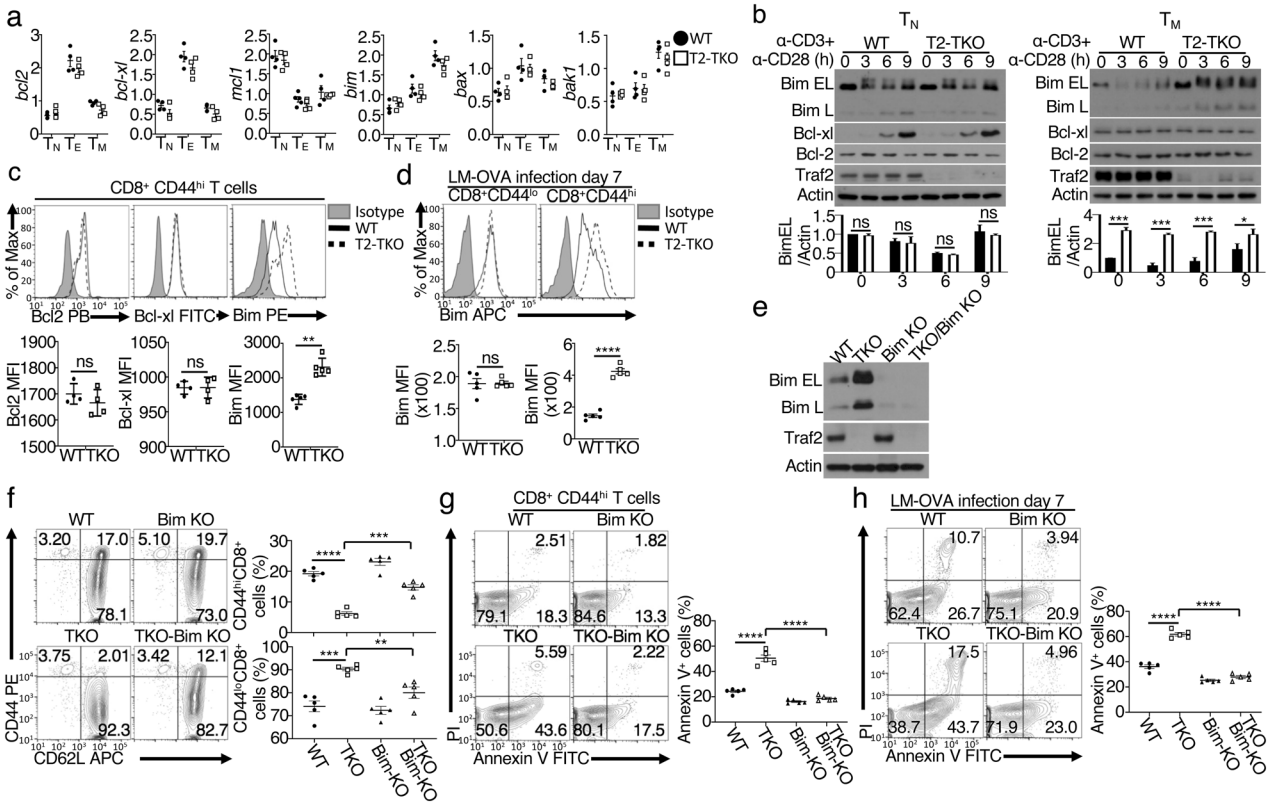

Fig. 4 TRAF2 controls the fate of Bim and supports the survival of effector and memory CD8 T cells. **a** QPCR analysis of the indicated genes in naïve (T_N) or in vitro-differentiated effector (T_E), and memory (T_M) CD8 T cells ($n = 4$). **b** Immunoblot analysis of the indicated proteins in whole-cell lysates of naïve (T_N) or in vitro-differentiated memory (T_M) CD8 T cells stimulated with plate-bound anti-CD3 plus anti-CD28 antibodies for the indicated durations. Quantification of Bim EL bands is presented as the ratio of the Bim EL level to the Actin level (lower). **c** Flow cytometric analysis, based on intracellular staining, of the indicated proteins in memory-like ($CD44^{hi}$) CD8 T cells in the spleens of 8-week-old wild-type (WT) and *Traf2*-TKO mice ($n = 4$). **d** Flow cytometric analysis of intracellular Bim in naïve ($CD44^{lo}$) or memory ($CD44^{hi}$) CD8 T cells from the spleens of WT and *Traf2*-TKO mice 7 days after infection with LM-OVA ($n = 5$). **e** Immunoblot analysis of Traf2 and Bim isoforms in whole-cell lysates of in vitro-differentiated memory CD8 T cells from wild-type (WT), *Traf2*-TKO (TKO), Bim KO, and *Traf2*-TKO/Bim KO mice. Flow cytometric analysis of the percentages of naïve ($CD44^{lo}$) and memory ($CD44^{hi}$) CD8 T cells (**f**) and the percentage of apoptotic cells within the memory ($CD44^{hi}$) CD8 T cell population (**g**) in the spleens of 8-week-old WT, *Traf2*-TKO (TKO), Bim KO (WT-Bim KO), and *Traf2*-TKO/Bim KO mice ($n = 5$). **h** Flow cytometric analysis of apoptosis in splenic memory ($CD44^{hi}$) CD8 T cells from the indicated mice 7 days after infection with LM-OVA ($n = 5$). Data are representative of two (**e**, **h**) or three (**a**–**d**, **f**, **g**) independent experiments. Data in summary graphs are presented as the mean ± SEM values based on multiple mice (each symbol represents a mouse), and *p* values were determined by unpaired Student's *t* test. *$p < 0.05$; **$p < 0.01$; ***$p < 0.001$; ****$p < 0.0001$; ns not significant

showing impaired ERK phosphorylation in *Traf2*-TKO effector ($CD44^{hi}$) but not naïve ($CD44^{lo}$) CD8 T cells (Fig. 5e). In line with the dispensable role of TRAF2 in CD4 T cell survival, TRAF2 deficiency did not affect ERK phosphorylation in naïve or memory CD4 T cells (Supplementary Fig. 4).

ERK is a kinase that mediates TCR/CD28-stimulated Bim degradation, which is crucial for T cell survival.[9,11,35] Consistent with this role, we found that the impairment of ERK phosphorylation in TRAF2-deficient effector and memory CD8 T cells was associated with an increased level of Bim expression (Fig. 5c). Furthermore, TCR/CD28-stimulated Bim downregulation was impaired in *Traf2*-TKO CD8 memory T cells and in wild-type CD8 T cells incubated with the ERK inhibitor U0126 (Fig. 5f). These results suggest that TRAF2 is crucial for TCR/CD28-stimulated activation of MEK/ERK signaling, which may constitute a major mechanism by which TRAF2 mediates effector/memory CD8 T cell survival.

Restoration of ERK signaling rescues the survival of TRAF2-deficient effector/memory CD8 T cells

To directly examine whether the impaired ERK activation in TRAF2-deficient CD8 T cells is responsible for their survival, we used a genetic approach to restore ERK signaling in TRAF2-deficient T cells. We employed a transgenic mouse strain expressing a constitutively active form of MEK1, $MEK1^{DD}$, via the Cre-loxP system ($R26Stop^{FL}MEK1^{DD}$).[36] By crossing $R26Stop^{FL}$-$MEK1^{DD}$ mice with CD4-Cre mice, we were able to generate T cell-conditional $MEK1^{DD}$ mice. We also crossed *Traf2*-TKO mice with $R26Stop^{FL}MEK1^{DD}$ mice to generate mice with T cell-conditional deletion of *Traf2* and expression of $MEK1^{DD}$ (TKO-$MEK1^{DD}$) and control mice. As expected, ERK phosphorylation was defective in *Traf2*-TKO memory CD8 T cells but was restored in TKO-$MEK1^{DD}$ memory CD8 T cells (Fig. 5g). More importantly, while *Traf2*-TKO memory CD8 T cells had a defect in TCR/CD28-stimulated Bim downregulation, this defect was completely corrected in TKO-$MEK1^{DD}$ memory CD8 T cells (Fig. 5g). Consistent with this result, T cell-specific expression of $MEK1^{DD}$ in *Traf2*-TKO mice rescued the survival of CD8 memory T cells. While *Traf2*-TKO mice had significant reductions in the frequency and absolute number of CD8 T cells compared to those in wild-type mice, this phenotype was completely reversed in TKO-$MEK1^{DD}$ mice (Fig. 5h). In addition, $MEK1^{DD}$ transgene expression restored the frequency and absolute number of memory-like ($CD44^{hi}$) CD8 T cells in *Traf2*-TKO mice (Fig. 5i). Mechanistically, $MEK1^{DD}$ expression prevented the aberrant apoptosis of *Traf2*-TKO effector and memory CD8 T cells under both homeostatic (Fig. 5j) and LM-OVA infection

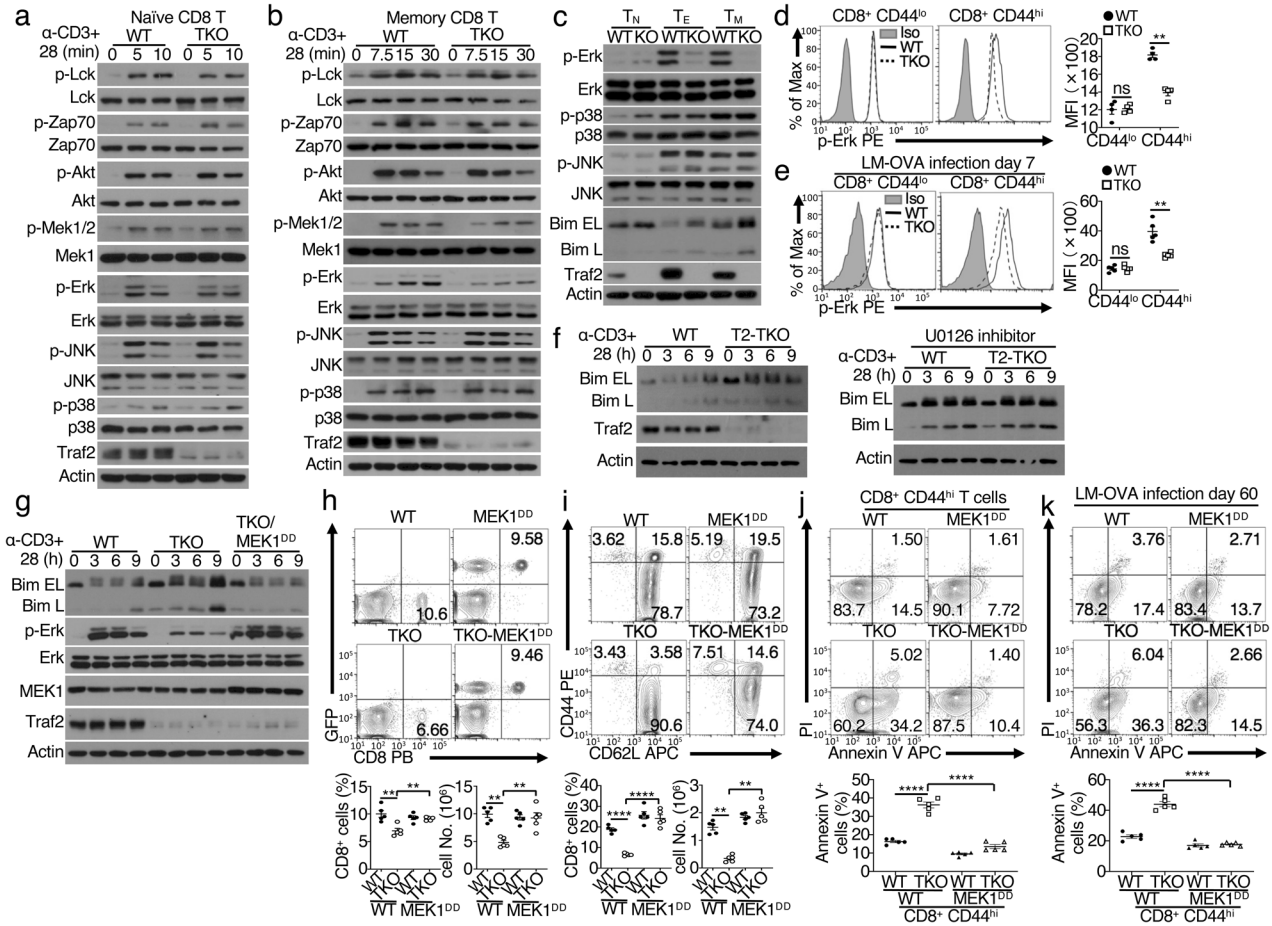

Fig. 5 TRAF2 is required for ERK activation. Immunoblot analysis of the indicated phosphorylated (p-) and total proteins in whole-cell lysates of wild-type (WT) and *Traf2*-TKO naïve (**a**) or memory (**b**) CD8 T cells stimulated for the indicated durations with anti-CD3 plus anti-CD28 antibodies. **c** Immunoblot analysis of the indicated phosphorylated (p-) or total proteins in whole-cell lysates of naïve (T_N) or in vitro-differentiated effector (T_E), and memory (T_M) WT and *Traf2*-TKO CD8 T cells. Flow cytometric analysis of phosphorylated ERK (p-ERK) in naïve ($CD44^{lo}$) or memory-like ($CD44^{hi}$) CD8 T cells in WT or *Traf2*-TKO mice that were either uninfected (**d**) or 7 days after infection with LM-OVA ($n = 5$) (**e**). **f** Immunoblot analysis of Bim isoforms in WT and *Traf2*-TKO memory CD8 T cells stimulated with plate-bound anti-CD3 plus anti-CD28 antibodies in the absence (left) or presence (right) of the MEK1 inhibitor U0126. **g** Immunoblot analysis of phosphorylated (p-) and total protein in whole-cell lysates of WT, *Traf2*-TKO (TKO), and *Traf2*-TKO/$MEK1^{DD}$ (TKO/$MEK1^{DD}$) memory CD8 T cells stimulated for the indicated durations with anti-CD3 plus anti-CD28 antibodies. Flow cytometric analysis of the percentages and absolute numbers of CD8 T cells (**h**) and naïve ($CD44^{lo}$) and memory-like ($CD44^{hi}$) CD8 T cells (**i**) in the spleens of 8-week-old WT, *Traf2*-TKO (TKO), $MEK1^{DD}$, and *Traf2*-TKO/$MEK1^{DD}$ (TKO-$MEK1^{DD}$) mice ($n = 5$). Flow cytometric analysis of apoptosis in splenic memory-like ($CD44^{hi}$) CD8 T cells from uninfected mice (**j**) and splenic memory ($CD44^{hi}$) CD8 T cells in mice of the indicated genotypes 60 days after infection with LM-OVA (**k**) ($n = 5$). Data are representative of two (**f**, **k**) or three (**a**–**e**, **g**–**j**) independent experiments. Summary data are presented as the mean ± SEM values based on multiple mice, and *p* values were determined by unpaired Student's *t* test. $^{**}p < 0.01$; $^{****}p < 0.0001$; ns not significant

(Fig. 5k) conditions. These results provide genetic evidence that TRAF2 regulates memory CD8 T cell survival by facilitating MEK/ERK signaling.

TRAF2 facilitates ERK activation by regulating Tpl2

The mechanism by which ERK is activated by TCR/CD28 signals in effector and memory CD8 T cells is not well understood, although both Ras-dependent and Ras-independent pathways have been implicated.[37,38] We found that TRAF2 deficiency did not influence TCR/CD28-stimulated activation of BRAF or RAF1, downstream kinases of Ras, suggesting the involvement of a different mechanism in TRAF2-mediated ERK regulation (Supplementary Fig. 5). Another upstream kinase known to target the MEK/ERK signaling pathway is Tpl2.[21] Tpl2 is best known as a MAP3K that responds to signals from innate immune receptors, particularly pattern recognition receptors (PRRs).[21] However, Tpl2 has also been shown to play a role in regulating T cell functions, especially CD4 T cell differentiation.[39] The function of Tpl2 is tightly controlled by the NF-κB1 precursor protein p105, which acts as both the inhibitor and stabilizer of Tpl2.[19,20] PRR signals induce phosphorylation-dependent p105 degradation, thereby triggering Tpl2 activation; activated Tpl2 activates the MEK/ERK pathway but is then degraded due to its instability when not complexed with p105. Thus, while p105 degradation is required for Tpl2 activation under normal conditions, Tpl2 is lost in p105-deficient cells, leading to defective ERK activation.[19–21]

Freshly prepared effector and memory CD8 T cells expressed markedly higher levels of Tpl2 and p105 proteins than naïve CD8 T cells, and this effect was associated with increased TRAF2 expression and ERK phosphorylation (Fig. 6a). Interestingly, TRAF2 deficiency resulted in profoundly reduced expression levels of Tpl2 and p105 in effector and memory but not naïve CD8 T cells (Fig. 6b). This phenotype appeared to be due to posttranslational regulation of Tpl2 and p105, since wild-type and *Traf2*-TKO CD8 T cells had comparable mRNA expression levels of Tpl2 and p105 (Fig. 6c). These results suggest that reduced Tpl2 expression may

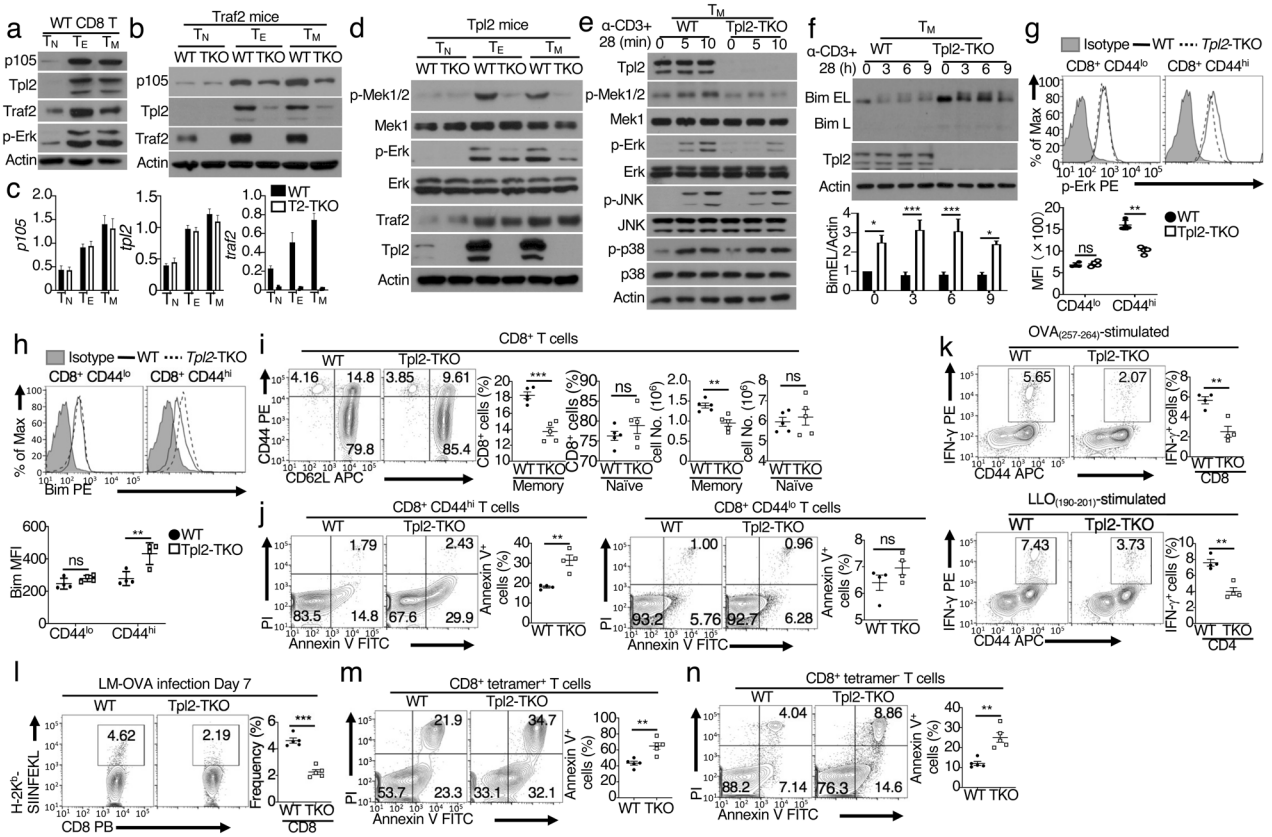

Fig. 6 TRAF2 regulates ERK signaling by stabilizing the p105/Tpl2 complex. Immunoblot analysis of the indicated proteins in whole-cell lysates of naïve (T_N) or in vitro-differentiated effector (T_E), and memory (T_M) CD8 T cells derived from WT mice (**a**) and from wild-type (WT) and *Traf2*-TKO (TKO) mice (**b**). **c** QPCR analysis of the indicated genes in naïve (T_N) and in vitro-differentiated effector (T_E) and memory (T_M) CD8 T cells ($n = 4$). **d** Immunoblot analysis of the indicated proteins in whole-cell lysates of naïve (T_N) and in vitro-differentiated effector (T_E), and memory (T_M) CD8 T cells from WT or *Tpl2*-TKO mice. **e**, **f** Immunoblot analysis of phosphorylated (p-) and total proteins in whole-cell lysates of WT and *Tpl2*-TKO memory CD8 T cells stimulated for the indicated durations with anti-CD3 plus anti-CD28 antibodies. The Bim EL band was quantified, and the level is presented as the ratio of Bim EL to Actin (**f**, lower). Flow cytometric analysis of p-ERK (**g**) and Bim (**h**) levels in naïve ($CD44^{lo}$) and memory ($CD44^{hi}$) CD8 T cells from the spleens of 8-week-old WT and *Tpl2*-TKO mice ($n = 4$). **i** Flow cytometric analysis of the percentages and absolute numbers of naïve ($CD44^{lo}$) and memory-like ($CD44^{hi}$) CD8 T cells in the spleens of 8-week-old WT and *Tpl2*-TKO mice ($n = 5$). **j** Flow cytometric analysis of apoptotic cells within the memory-like ($CD44^{hi}$) and naïve ($CD44^{lo}$) CD8 T cell populations in the spleens of 8-week-old WT and *Tpl2*-TKO mice ($n = 4$). **k** Intracellular cytokine staining (ICS) and flow cytometric analysis of IFN-γ-producing CD8 and CD4 effector T cells in the spleens of WT and *Tpl2*-TKO mice 7 days after infection with LM-OVA ($n = 4$). Splenocytes were restimulated for 6 h with $OVA_{257–264}$ (for CD8 T cell stimulation) or $LLO_{190–204}$ (for CD4 T cell stimulation) peptide in the presence of monensin prior to analysis. **l** Flow cytometric analysis, using H-$2K^b$ OVA (SIINFKL) tetramers, of the percentage of antigen-specific CD8 T cells in the spleens of WT and *Tpl2*-TKO mice 7 days after infection with LM-OVA ($n = 5$). **m**, **n** Flow cytometric analysis of apoptotic cells within the H-$2K^b$ OVA tetramer-positive and H-$2K^b$ OVA tetramer-negative CD8 T cell populations in the spleens of WT and *Tpl2*-TKO mice 7 days after infection with LM-OVA ($n = 5$). Data are representative of two (**c**) or three (**a**, **b**, **d**–**n**) independent experiments. Summary data are presented as the mean ± SEM values based on multiple mice. Summary data are presented as the mean ± SEM values based on multiple mice, and *p* values were calculated by Student's *t* test. *$p < 0.05$; **$p < 0.01$; ***$p < 0.001$; ns not significant

contribute to the MEK/ERK signaling defect in *Traf2*-TKO effector/memory CD8 T cells. To further examine this possibility, we generated mutant mice carrying T cell-conditional deletion of the Tpl2-encoding gene *Map3k8* (hereafter called *Tpl2*-TKO mice). Tpl2 deficiency in effector and memory CD8 T cells caused severe defects in the phosphorylation of MEK1/2 and ERK1/2 under steady-state conditions (Fig. 6d). To further confirm that Tpl2 regulates TCR/CD28-stimulated MEK/ERK activation, we rested the memory CD8 T cells in serum-free RPMI 1640 medium to reduce steady-state signaling and then restimulated the cells with anti-CD3 plus anti-CD28 antibodies. Under these conditions, Tpl2-deficient memory CD8 T cells exhibited impairment of TCR/CD28-stimulated phosphorylation of MEK1/2 and ERK1/2 with little or no effect on the activation of JNK and p38 (Fig. 6e). Importantly, Tpl2 deficiency also blocked TCR/CD28-stimulated Bim downregulation in CD8 memory T cells (Fig. 6f). Furthermore, *Tpl2*-TKO memory but not naïve CD8 T cells exhibited impaired ERK phosphorylation and increased Bim expression under in vivo homeostatic conditions (Fig. 6g, h). These results were reminiscent of those observed in *Traf2*-TKO CD8 T cells.

In line with the results of these signaling studies, flow cytometric analysis revealed a significantly reduced frequency and absolute number of CD8 but not CD4 memory-like T cells in *Tpl2*-TKO mice (Fig. 6i and Supplementary Fig. 6). Consistent with this pattern, *Tpl2*-TKO mice exhibited an increased frequency of apoptotic cells within the memory-like ($CD44^{hi}$) but not the naïve ($CD44^{lo}$) CD8 T cell population (Fig. 6j). In addition, Tpl2 deficiency reduced the frequency of antigen-specific memory CD8 T cells during the immune response to LM-OVA infection, as measured based on IFN-γ production upon in vitro restimulation with the LM-OVA-specific antigens $OVA_{257–264}$ and $LLO_{190–204}$ (Fig. 6k). Moreover, the frequency of OVA tetramer-specific CD8 T cells was also reduced in *Tpl2*-TKO mice (Fig. 6l). Compared to wild-type mice, *Tpl2*-TKO mice exhibited a drastically increased frequency of

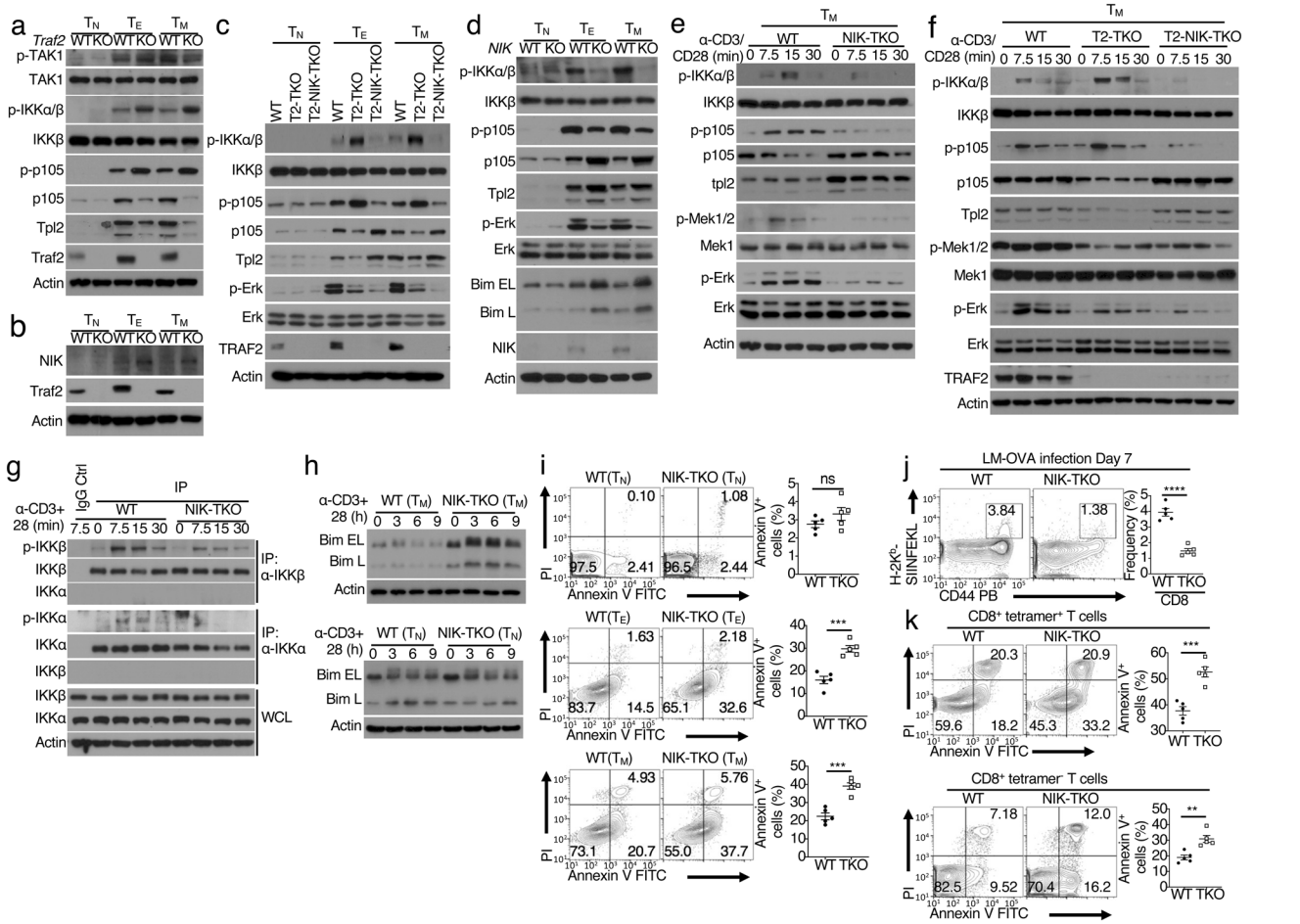

Fig. 7 NIK is a key regulator of Tpl2-ERK signaling in effector and memory CD8 T cells. Immunoblot analysis of the indicated phosphorylated (p-) and total proteins in whole-cell lysates of naïve (T_N) and in vitro-differentiated effector (T_E) and memory (T_M) CD8 T cells from wild-type (WT) and *Traf2*-TKO (KO) mice (**a**, **b**) and from WT, *Traf2*-TKO (T2-TKO), and Traf2-NIK double TKO (T2-NIK-TKO) mice (**c**). **d** Immunoblot analysis of phosphorylated (p-) and total proteins in whole-cell lysates of naïve (T_N) and in vitro-differentiated effector (T_E) and memory (T_M) CD8 T cells from WT and NIK-TKO (KO) mice. Immunoblot analysis of phosphorylated (p-) and total proteins in whole-cell lysates of in vitro-differentiated memory (T_M) CD8 T cells derived from WT and NIK-TKO mice (**e**) and from WT, *Traf2*-TKO (T2-TKO), and Traf2-NIK double TKO (T2-NIK-TKO) mice (**f**), stimulated with anti-CD3 plus anti-CD28 antibodies for the indicated durations. **g** Immunoblot analyses of phosphorylated (p-) and total IKK protein isolated by immunoprecipitation under denaturing conditions with IKKα or IKKβ antibodies or directly from whole-cell lysates (WCL) of WT and NIK-TKO memory (T_M) CD8 T cells stimulated with anti-CD3 plus anti-CD28 antibodies. IgG immunoprecipitation was included as a negative control. **h** Immunoblot analysis of the indicated proteins in whole-cell lysates of WT and NIK-TKO memory (T_M) and naïve (T_N) CD8 T cells stimulated for the indicated durations with anti-CD3 plus anti-CD28 antibodies. **i** Flow cytometric analysis of apoptotic cells within the naïve (T_N) and in vitro-differentiated effector (T_E) and memory (T_M) CD8 T cell populations derived from WT and NIK-TKO mice ($n = 5$). Flow cytometric analysis of the percentage of antigen (OVA)-specific CD8 T cells using H-2K^b OVA (SIINFKL) tetramers (**j**) and apoptotic cells within the tetramer$^+$ and tetramer$^-$ CD8 T cell populations (**k**) in the spleens of WT and NIK-TKO mice 7 days after infection with LM-OVA ($n = 5$). Data are representative of two (**f**, **j**, **k**) or three (**a**–**e**, **g**–**i**) independent experiments. Summary data are presented as the mean ± SEM values based on multiple mice. *p* values were determined by unpaired Student's *t* test (**i**–**k**). $^{**}p < 0.01$; $^{***}p < 0.001$; $^{****}p < 0.0001$; ns not significant

apoptotic CD8 T cells within the OVA tetramer$^+$ antigen-specific memory cell population (Fig. 6m). Tpl2 deficiency also promoted apoptosis in the OVA tetramer$^-$ CD8 T cell population, although less profoundly than in the corresponding OVA tetramer$^+$ population, which was likely due to the presence of memory CD8 T cells specific for other LM-OVA epitopes (Fig. 6n). Collectively, these results demonstrate an important role for Tpl2 in regulating the survival of effector and memory CD8 T cells, showing the functional significance of TRAF2-mediated Tpl2 regulation.

TRAF2 regulates the Tpl2-ERK signaling axis by controlling NIK function

The molecular mechanism underlying Tpl2 activation in T cells, particularly effector/memory CD8 T cells, is obscure. We and others have previously shown that TLR-stimulated Tpl2 activation in macrophages requires IKK, which mediates phosphorylation-dependent p105 degradation and Tpl2 liberation.[22,23] Interestingly, we found that TRAF2 deficiency greatly enhanced the steady-state level of IKK activation in effector and memory CD8 T cells (Fig. 7a). TRAF2 deficiency did not promote activation of TAK1, a known IKK-activating kinase, suggesting the involvement of a different kinase (Fig. 7a). In this regard, a known target of TRAF2 is NIK. Under normal conditions, NIK is constantly degraded via ubiquitination mediated by an E3 ligase complex composed of TRAF2, TRAF3, and a cIAP protein (cIAP1 or cIAP2), and genetic deficiency in either TRAF2 or TRAF3 results in NIK accumulation and activation[40]. Indeed, TRAF2 deficiency profoundly increased the protein level of NIK in effector and memory CD8 T cells (Fig. 7b).

To investigate the functional significance of NIK deregulation in TRAF2-deficient CD8 T cells, we generated mice harboring deletion of both Traf2 and NIK (*Traf2-NIK*-TKO mice). Remarkably, NIK deletion strongly inhibited IKK activation and reduced p105 phosphorylation, coupled with a drastic increase in the p105 protein level (Fig. 7c). Consistent with the role of p105 in mediating Tpl2 stabilization, the level of Tpl2 was similarly increased upon NIK deletion (Fig. 7c). Notably, restoration of Tpl2 expression in Traf2/NIK double-deficient CD8 T cells did not lead to rescue of ERK activation (Fig. 7c). This result was not surprising, since impaired p105 degradation is expected to block Tpl2 activation despite stabilization of the p105/Tpl2 complex.[21] These results suggest that deregulated NIK activation in TRAF2-deficient CD8 effector/memory T cells contributes to aberrant activation of IKK and degradation of p105 and Tpl2.

Previous studies suggest that TRAF1 mediates ERK signaling and Bim downregulation induced by the TNFR 4-1BB in activated and memory CD8 T cells.[41] Since TRAF2 has also been implicated in the regulation of 4-1BB signaling,[42] we examined the effect of TRAF2 deficiency on 4-1BB-mediated signaling in memory CD8 T cells. TRAF2-deficient memory CD8 T cells were defective in Erk phosphorylation stimulated by an anti-4-1BB agonist antibody (Supplementary Fig. 7a). However, TRAF2 deficiency did not inhibit anti-4-1BB-induced phosphorylation of several other signaling molecules, including Akt, p38, and JNK, and even promoted the phosphorylation of IKKβ (Supplementary Fig. 7a). Furthermore, impaired Erk signaling was associated with drastic loss of the upstream kinase Tpl2 (Supplementary Fig. 7a). These results were reminiscent of the effect of TRAF2 deficiency on TCR/CD28 signaling (Figs. 5b and 7f). We further showed that TRAF2 deficiency promoted the apoptosis of memory CD8 T cells even when 4-1BB and another TNFR, OX40, were blocked by monoclonal antibodies (Supplementary Fig. 7b, c), suggesting that TRAF2-mediated memory CD8 T cell survival is outside the regulation of 4-1BB signaling.

NIK is a physiological mediator of Tpl2-ERK signaling in effector/memory CD8 T cells

NIK is known as a kinase that mediates noncanonical NF-κB activation induced by TNFR superfamily members.[43] NIK activation is typically mediated through TNFR-stimulated degradation of TRAF3 and, in some cases, TRAF2. Interestingly, TCR/CD28-mediated NIK induction accompanied by effector and memory CD8 T cell generation was associated with loss of cIAP1 and cIAP2 but not TRAF2 or TRAF3, suggesting an atypical mechanism of activation involving loss of cIAPs (Supplementary Fig. 8). NIK deficiency severely impaired steady-state IKK activation in freshly prepared effector and memory CD8 T cells (Fig. 7d). Consistent with this result, NIK deficiency also resulted in reduced p105 phosphorylation and increased total protein levels of p105 and Tpl2, which were associated with impaired ERK phosphorylation and Bim accumulation (Fig. 7d). Notably, this function of NIK was unlikely to be mediated by noncanonical NF-κB, since CD8 T cells defective in noncanonical NF-κB activation due to expression of a processing-defective p100 mutant, Lym1,[44] displayed similar levels of p105/Tpl2 expression and ERK phosphorylation (Supplementary Fig. 9a).

To further confirm that NIK mediates TCR/CD28-stimulated Tpl2-ERK signaling, we rested CD8 T cells and restimulated them with anti-CD3 plus anti-CD28 antibodies. In naïve CD8 T cells, NIK deficiency did not affect anti-CD3/anti-CD28-stimulated IKK activation, p105 phosphorylation, or ERK phosphorylation (Supplementary Fig. 9b), in line with the extremely low expression level of NIK in naïve CD8 T cells (Fig. 7b). In contrast, in memory CD8 T cells, NIK deficiency severely attenuated IKK activation, especially at late time points (15 and 30 min) (Fig. 7e). Consistent with this finding, NIK deficiency also inhibited TCR/CD28-stimulated phosphorylation and degradation of p105 and activation of Tpl2, as evidenced by the defective phosphorylation of its downstream targets MEK1/2 and ERK1/2 (Fig. 7e). Furthermore, while *Traf2*-TKO memory CD8 T cells exhibited hyperphosphorylation of IKK and p105 after TCR/CD28 stimulation, NIK deletion blocked these signaling events (Fig. 7f). These results suggested a crucial role for NIK in mediating TCR/CD28-stimulated IKK activation, p105 phosphorylation, and Tpl2-ERK signaling in memory but not naïve CD8 T cells. NIK is thought to selectively target IKKα in the noncanonical NF-κB signaling pathway.[17] To further examine NIK-dependent IKK activation in memory CD8 T cells, we isolated IKKα and IKKβ under denaturing conditions (to disrupt the IKK complex) and then detected the activation of IKKα and IKKβ by phosphoimmunoblotting. Interestingly, in memory CD8 T cells, NIK was required for TCR/CD28-stimulated phosphorylation of both IKKα and IKKβ (Fig. 7g).

We next examined the function of NIK in regulating Bim degradation and CD8 T cell survival. In line with its dispensable role in ERK activation in naïve CD8 T cells (Supplementary Fig. 9b), NIK deficiency did not affect TCR/CD28-stimulated Bim degradation in naïve CD8 T cells (Fig. 7h). In contrast, NIK deficiency attenuated TCR/CD28-stimulated Bim degradation and also increased the steady-state level of Bim in memory CD8 T cells (Fig. 7h). Consistent with these effects, NIK deficiency profoundly promoted the apoptosis of effector and memory but not naïve CD8 T cells under in vitro conditions (Fig. 7i). The function of NIK in mediating effector/memory CD8 T cell survival was further demonstrated in vivo using the LM-OVA infection model. Seven days after LM-OVA infection, NIK-TKO mice had a significantly lower level of antigen-specific CD8 effector T cells than did wild-type control mice, as demonstrated based on flow cytometry using a tetramer loaded with the OVA peptide SIIFEKL (Fig. 7j). This phenotype was associated with increased apoptosis of tetramer$^+$ CD8 T cells (Fig. 7k, upper panel). In addition, NIK-TKO mice exhibited an increased frequency of apoptotic cells within the SIINFEKL tetramer-negative population (Fig. 7k, lower panel); however, this result was obviously due to the presence of effector CD8 T cells specific for other LM-OVA epitopes, since parallel analysis revealed increased apoptosis in CD44^{hi} (including effector T cells activated by all epitopes) but not CD44^{lo} NIK-TKO CD8 T cells (Supplementary Fig. 10).

DISCUSSION

In the present study, we demonstrated that TRAF2 regulates antigen-specific T cell responses and protective immunity by maintaining a survival signaling axis in effector and memory CD8 T cells. This signaling axis involves NIK-dependent activation of Tpl2 and its downstream kinases MEK1/2 and ERK1/2, leading to posttranslational downregulation of the proapoptotic protein Bim. NIK mediates activation of IKK and phosphorylation of the Tpl2 inhibitory protein p105, a mechanism that triggers p105 degradation and Tpl2 activation. However, while NIK is normally required for TCR/CD28-stimulated Tpl2-ERK signaling, aberrant NIK accumulation in TRAF2-deficient CD8 T cells causes constitutive degradation of p105 and Tpl2, resulting in a severe defect in MEK-ERK signaling in effector/memory CD8 T cells and greatly reducing their survival.

TRAF2 is known as an adapter protein involved in signaling from TNFR superfamily members.[14] However, emerging evidence suggests the involvement of TRAF2 in other cellular processes. A recent study suggests that TRAF2 regulates CD8 T cell homeostasis by modulating the sensitivity of memory-like CD8 T cells to IL-15.[15] In agreement with this previous study, we found that TRAF2 deficiency partially inhibited the proliferation of in vitro-differentiated memory CD8 T cells. Interestingly, however, our study did not reveal an effect of TRAF2 deficiency on IL-15-induced phosphorylation of AKT and STAT5 in either memory or naïve CD8 T cells, although previous work identified

hyperactivation of AKT in TRAF2-deficient thymocytes. These findings suggest that TRAF2 may regulate a downstream signaling event important for CD8 T cell responses to both IL-15 and antigens. Indeed, our present study demonstrated a role for TRAF2 in maintaining TCR/CD28-stimulated ERK activation. In line with the role of ERK in mediating Bim degradation and T cell survival,[9,11,35] we found that TRAF2 deficiency promoted Bim accumulation and apoptosis in effector and memory CD8 T cells under both in vivo and in vitro conditions. Transgenic expression of a constitutively active form of the ERK kinase MEK1^{DD} rescued the survival of TRAF2-deficient CD8 T cells, emphasizing the functional significance of TRAF2-mediated ERK signaling. Furthermore, the survival of TRAF2-deficient T cells was rescued by deletion of Bim. These findings establish TRAF2 as a pivotal regulator of the survival signaling network in effector and memory CD8 T cells. Given the role of ERK in mediating both the survival and proliferation of CD8 T cells,[35] it is possible that the hypoproliferative phenotype of TRAF2-deficient memory CD8 T cells is also attributed to an ERK signaling defect.

We found that TRAF2 was not required for TCR/CD28-stimulated activation of BRAF or RAF1 but was crucial for regulating another ERK-upstream kinase, Tpl2. We obtained genetic evidence indicating that Tpl2 is indispensable for TCR/CD28-stimulated ERK activation in effector and memory CD8 T cells and for their survival. Interestingly, Tpl2 expression is low in naïve CD8 T cells and drastically upregulated in effector/memory CD8 T cells. We and others have previously shown that Tpl2 is tightly regulated by the IκB-like protein p105, which functions as both an inhibitor and a stabilizer of Tpl2.[19–21] In innate immune cells, Tpl2 activation by TLRs involves IKK-mediated phosphorylation and degradation of p105.[22,23] However, the mechanism by which Tpl2 is activated by TCR signaling has historically been elusive. Our present study identified NIK as a pivotal upstream kinase mediating TCR/CD28-stimulated IKK activation and p105 phosphorylation, leading to Tpl2-ERK activation in effector/memory CD8 T cells. Interestingly, TRAF2 deficiency did not inhibit TCR/CD28-stimulated p105 phosphorylation but drastically reduced the expression levels of both p105 and Tpl2, the latter of which apparently contributes to the Tpl2-ERK signaling defect in TRAF2-deficient CD8 T cells. Our data suggest that the loss of p105 and Tpl2 in TRAF2-deficient T cells is due to aberrant accumulation of NIK. Thus, maintenance of the NIK-Tpl2-ERK signaling axis by TRAF2 is crucial for Tpl2-ERK signaling and the survival of effector/memory CD8 T cells.

NIK is a kinase known for the induction of noncanonical NF-κB signaling by TNFR superfamily members.[17] By employing a mutant mouse strain expressing a processing-defective p100 mutant, Lym1, we demonstrated that NIK-mediated Tpl2-ERK activation was independent of noncanonical NF-κB activation. Thus, in effector/memory T cells, NIK targets two major signaling pathways: the noncanonical NF-κB pathway and the Tpl2-ERK pathway. A primary mechanism of NIK regulation is its ubiquitin-dependent degradation mediated by the cIAP-TRAF2-TRAF3 E3 ubiquitin ligase complex; NIK induction is typically mediated by degradation of TRAF3 and, in some cases, TRAF2.[17] Our study revealed that like TRAF2, TRAF3 is required for the control of NIK expression and TCR/CD28-stimulated activation of the Tpl2-ERK signaling axis and for the survival of effector/memory CD8 T cells (data not shown). Interestingly, we found that TCR/CD28-stimulated NIK induction was associated with loss of cIAP1 and cIAP2 instead of TRAF2 or TRAF3, suggesting an atypical mechanism mediating cIAP-TRAF2-TRAF3 complex disruption and NIK activation. Activated T cells are known to express several TNFRs, such as OX40, 4.1BB, and CD27, which are important for effector/memory T cell functions.[43,45] Future studies will examine whether NIK induction in T cells is mediated only by TCR/CD28 signaling or also involves the action of TNFRs. In conclusion, our work suggests a TRAF2-regulated NIK-Tpl2-ERK signaling axis that is crucial for the survival of effector/memory CD8 T cells.

MATERIALS AND METHODS

Mice

Traf2-flox mice were provided by Dr. Robert Brink (Garvan Institute of Medical Research)[46] and crossed with *Cd4*-Cre mice (The Jackson Laboratory) to generate age-matched *Traf2*$^{fl/fl}$*Cd4*-Cre (termed *Traf2*-TKO) and Traf2$^{fl/fl}$ (termed WT) mice. In some experiments, *Traf2*-TKO mice were further crossed with OT-I TCR-transgenic mice (The Jackson Laboratory), R26Stop^{FL}MEK1DD[36] (Map2k1*, The Jackson Laboratory, stock # 012352) mice, or Bcl2l11$^{tm1.1Ast}$ mice[47] (The Jackson Laboratory, stock # 004525). NIK (Map3k14)-floxed mice were provided by Genentech[48] and crossed with Cd4-Cre mice (The Jackson Laboratory) to generate age-matched NIK$^{fl/fl}$Cd4-Cre (termed NIK-TKO) and NIK$^{fl/fl}$ (termed WT) mice. B6.SJL mice (expressing the CD45.1 congenic marker) were obtained from the Jackson Laboratory. Mice with the conditionally targeted *Map3k8* allele (*Map3k8*$^{tm1b(KOMP)Wtsi}$) were generated by the Knockout Mouse Project (KOMP), and live mice were rederived using cryopreserved sperm from the KOMP at the Genetically Engineered Mouse Facility of The University of Texas MD Anderson Cancer Center. *Map3k8*-floxed mice were generated by crossing *Map3k8*$^{tm1b(KOMP)Wtsi}$ mice with FLP deleter (Rosa26-FLPe) mice (Jackson Lab) and then crossing these mice with Cd4-Cre mice to produce *Map3k8*$^{fl/fl}$Cd4-Cre (termed *Tpl2*-TKO) and *Map3k8*$^{+/+}$Cd4-Cre (termed WT) mice. Nfkb2^{lym1} mice were provided by R. Starr (Walter and Eliza Hall Institute of Medical Research), and Nfkb2$^{lym1/+}$ heterozygous mice were used in experiments since they display a strong phenotype of impaired noncanonical NF-κB activation and function.[44] The Nfkb2$^{lym1/+}$ mice were on a 129 genetic background, and all other mouse strains were on a C57BL/6 genetic background. Sex- and age-matched KO and wild-type control mice were used in experiments. Genotyping was performed using the primers listed in Table S1. Mice were maintained in the specific pathogen-free facility at The University of Texas MD Anderson Cancer Center, and all animal experiments were conducted in accordance with protocols approved by the Institutional Animal Care and Use Committee.

Antibodies and reagents

The antibodies and reagents used in this study are listed in Table S2.

T cell isolation and differentiation in vitro

CD8$^+$ T cells were isolated from splenocytes and lymph node cells with anti-CD8 antibody conjugated magnetic beads (Miltenyi Biotec). Naïve T cells were further purified by FACS sorting based on the CD44^{lo} CD62L^{hi} surface marker phenotype. For in vitro generation of effector and memory T cells, naïve CD8 T cells were activated with plate-bound anti-CD3 (5 μg/ml) (anti-mouse CD3, Invitrogen, Cat# 14-0031-82) and anti-CD28 (0.5 μg/ml) (anti-mouse CD28, Invitrogen, Cat# 16-0281-82) antibodies for 3 days in the presence of IL-2 (10 ng/ml). The activated T cells were plated in RPMI 1640 medium containing 10 ng/ml IL-2 (for effector T cell differentiation) or 20 ng/ml IL-15 (for memory T cell differentiation) for 3 days. To isolate CD8 T cells from OT-I mice, single cell suspensions of splenocytes were incubated for 48 h in IL-2-containing medium in the presence of $OVA_{257–264}$ peptide (SIINFEKL, Genemed Synthesis) and were subsequently purified with Lymphocyte Cell Separation Medium (Cedarlane, Cat# CL5035) to remove non-T cells and dead cells. The purified T cells were cultured in the presence of IL-2 and IL-15 for an additional 3 days for differentiation into effector and memory T cells, respectively.

Listeria monocytogenes infection

The indicated age- and sex-matched wild-type and conditional KO mice (8–10 weeks old) were infected intravenously with 5×10^4 colony-forming units (CFU) of OVA-expressing recombinant

L. monocytogenes (LM-OVA)[49] (provided by Hao Shen, University of Pennsylvania) on day 0. For evaluation of primary T cell responses, mice were sacrificed 7 days after bacterial infection, and splenocytes were collected for flow cytometric analysis of apoptosis and recall responses of listeriolysin O (LLO)-specific $CD4^+$ and ovalbumin (OVA)-specific $CD8^+$ effector T cells. In brief, splenocytes were stimulated with 10 μg/ml $LLO_{190–204}$ peptide (NEKYAQAYPNVS) or 10 μg/ml $OVA_{257–264}$ peptide (SIINFEKL) in the presence of monensin for 6 h, and intracellular IFN-γ staining and flow cytometric analysis were then performed. For evaluation of memory T cell responses, mice were reinfected with 1×10^6 cfu of LM-OVA on day 60 after the primary infection. Three days later, mice were sacrificed, and splenocytes were collected for flow cytometric analysis of memory T cells rapidly activated by LM-OVA reinfection. To determine the bacterial load in infected mice, spleens, and livers were collected at the indicated time points and homogenized in 10 ml of 0.2% (vol/vol) NP-40 in PBS, and the organ homogenates were serially diluted and plated on brain heart infusion agar plates to determine the bacterial load. Bacterial colonies were counted after incubation at 37 °C for 24 h and are presented as the number of bacteria per organ or tissue.

To examine infection-mediated protective immunity, age- and sex-matched wild-type and conditional KO mice (6–8 weeks old) were infected intravenously with a low dose (1×10^4 cfu/mouse) of LM-OVA on day 0. Thirty days later, mice were rechallenged with a lethal dose (2×10^6 cfu/mouse) of LM-OVA and monitored for survival.

B16-OVA tumor model

Traf2-TKO mice and age- and sex-matched wild-type control mice (6–8 weeks old) were infected with a low dose (1×10^4 cfu/mouse) of LM-OVA on day 0. After 40 days, mice were injected s.c. with 8×10^5 B16-OVA murine melanoma cells and monitored for tumor growth and survival. Mice with tumor volumes measuring 225 mm^2 were considered moribund and sacrificed according to protocols approved by the Institutional Animal Care and Use Committee of the University of Texas MD Anderson Cancer Center.

Flow cytometry and intracellular cytokine staining (ICS)

For analysis of surface markers, cells were stained in RPMI 1640 containing 2% (vol/vol) FBS, unless noted otherwise, with antibodies specific for CD4 (RM4-5), CD8α (53–6.7), CD44 (1M7), CD62L (MEL-14), CD45.1 (A20), and CD45.2 (104). OVA peptide (SIINFEKL)-loaded mouse H-2Kb tetramers were obtained from the US National Institutes of Health Tetramer Facility. For ICS, T cells were stimulated for 4–6 h with specific peptides in the presence of monensin, fixed, and permeabilized using BD Phosflow Fix Buffer I/III (BD Biosciences), and stained intracellularly with antibodies specific for Bcl2, Bcl-xl, Bim, and p-ERK. All antibodies were used at a 1:200 dilution unless otherwise stated. Cells were analyzed using an LSRFortessa flow cytometer (BD), and data were analyzed with FlowJo software. Analysis of the stained populations was performed by gating on single cells.

Apoptotic cell detection

Apoptotic cells were detected with an Annexin V Apoptosis Detection Kit (BD Biosciences). Cells were stained with annexin V and PI for 15 min at RT according to the manufacturer's instructions and analyzed by flow cytometry.

ELISA and qRT-PCR

Sera from the indicated mice were analyzed by ELISA using a commercial assay system (eBioScience). For qRT-PCR, total RNA was isolated using TRIZOL reagent (Molecular Research Center, Inc.) and subjected to cDNA synthesis using RNase H reverse transcriptase (Invitrogen) and oligo (dT) primers. qRT-PCR was performed in triplicate using an iCycler Sequence Detection System (Bio-Rad) and iQTM SYBR Green Supermix (Bio-Rad). The expression levels of individual genes were calculated by a standard curve method and normalized to the expression level of *Actb*. The gene-specific PCR primers (all for mouse genes) are shown in Table S3.

Immunoblot, in vitro kinase and coimmunoprecipitation assays

T cells were lysed in RIPA buffer (50 mM Tris-HCl (pH 7.4), 150 mM NaCl, 1% (vol/vol) Nonidet P-40, 0.5% (vol/vol) sodium deoxycholate and 1 mM EDTA) and subjected to immunoblot and in vitro kinase assays as previously described.[50] Coimmunoprecipitation assays were performed essentially as described.[51] In brief, in vitro-differentiated memory CD8 T cells were starved overnight to reduce steady-state signaling and were then stimulated with anti-CD3 plus anti-CD28 antibodies for the indicated durations. The stimulated cells were lysed in RIPA buffer on ice for 10 min. After centrifugation, the cleared cell lysates (supernatants) were supplemented with SDS to a final concentration of 1% and heated for 5 min to denature proteins. Cell lysates were then diluted with RIPA buffer to reduce the SDS concentration to 0.1% and subjected to immunoprecipitation using the indicated antibodies prior to immunoblot analysis of the coprecipitated proteins.

Statistical analysis

Statistical analysis was performed using Prism 8 software (GraphPad Software). Comparisons between two groups were performed using unpaired two-tailed Student's *t* tests. For tumor growth curves, differences between groups were evaluated by two-way ANOVA with the Bonferroni correction. Survival data were plotted on Kaplan–Meier curves, and a log-rank (Mantel–Cox) test was performed. All statistical tests were justified as appropriate, and the data met the assumptions of the tests. The variances were similar between the groups under statistical comparison. The error bars indicate the standard error of the mean. All dots on plots represent biological replicates. Details are provided in the figure legends. The levels of significance are expressed as follows: $*p < 0.05$; $**p < 0.01$; $***p < 0.001$; $****p < 0.0001$.

ACKNOWLEDGEMENTS

We thank R Brink for the *Traf2*-flox mice, Genentech Inc. for the *Map3k14* flox mice and R Starr for the $Nfkb2^{lym1}$ mice. We also thank the personnel from the flow cytometry, DNA analysis, and animal facilities at The MD Anderson Cancer Center for technical assistance. This study was supported by grants from the National Institutes of Health (AI64639 and GM84459), and the core facilities of MD Anderson Cancer Center are supported by the NIH/NCI Cancer Center Support Grant (CCSG) P30CA016672.

AUTHOR CONTRIBUTIONS

X.X. designed and performed the research, prepared the figures, and wrote part of the manuscript; L.Z., Z.J., Y.L., M.G., X.Z., H.W., J.H.C., C.J.K., and X.C. contributed to performing the experiments; and S-C.S. supervised the work and wrote the manuscript.

ADDITIONAL INFORMATION

The online version of this article (https://doi.org/10.1038/s41423-020-00583-7) contains supplementary material.

Competing interests: The authors declare no competing interests.

REFERENCES

1. Durgeau, A., Virk, Y., Corgnac, S. & Mami-Chouaib, F. Recent advances in targeting CD8 T-Cell immunity for more effective cancer immunotherapy. *Front. Immunol.* **9**, 14 (2018).
2. Glimcher, L. H., Townsend, M. J., Sullivan, B. M. & Lord, G. M. Recent developments in the transcriptional regulation of cytolytic effector cells. *Nat. Rev. Immunol.* **4**, 900–911 (2004).

3. Cui, W. & Kaech, S. M. Generation of effector CD8+ T cells and their conversion to memory T cells. *Immunol. Rev.* **236**, 151–166 (2010).
4. Marsden, V. S. & Strasser, A. Control of apoptosis in the immune system: Bcl-2, BH3-only proteins and more. *Annu. Rev. Immunol.* **21**, 71–105 (2003).
5. Wojciechowski, S. et al. Bim/Bcl-2 balance is critical for maintaining naive and memory T cell homeostasis. *J. Exp. Med.* **204**, 1665–1675 (2007).
6. Hildeman, D. A. et al. Activated T cell death in vivo mediated by proapoptotic bcl-2 family member bim. *Immunity* **16**, 759–767 (2002).
7. Wojciechowski, S. et al. Bim mediates apoptosis of CD127(lo) effector T cells and limits T cell memory. *Eur. J. Immunol.* **36**, 1694–1706 (2006).
8. Weant, A. E. et al. Apoptosis regulators Bim and Fas function concurrently to control autoimmunity and CD8+ T cell contraction. *Immunity* **28**, 218–230 (2008).
9. Ley, R., Balmanno, K., Hadfield, K., Weston, C. & Cook, S. J. Activation of the ERK1/2 signaling pathway promotes phosphorylation and proteasome-dependent degradation of the BH3-only protein, Bim. *J. Biol. Chem.* **278**, 18811–18816 (2003).
10. Hubner, A., Barrett, T., Flavell, R. A. & Davis, R. J. Multisite phosphorylation regulates Bim stability and apoptotic activity. *Mol. Cell* **30**, 415–425 (2008).
11. O'Reilly, L. A. et al. MEK/ERK-mediated phosphorylation of Bim is required to ensure survival of T and B lymphocytes during mitogenic stimulation. *J. Immunol.* **183**, 261–269 (2009).
12. Ha, H., Han, D. & Choi, Y. TRAF-mediated TNFR-family signaling. *Curr. Protoc. Immunol.* **87**, 11.9D.1–11.9D.19 (2009).
13. Xie, P. TRAF molecules in cell signaling and in human diseases. *J. Mol. Signal.* **8**, 7 (2013).
14. Shi, J. H. & Sun, S. C. Tumor necrosis factor receptor-associated factor regulation of nuclear factor kappaB and mitogen-activated protein kinase pathways. *Front. Immunol.* **9**, 1849 (2018).
15. Villanueva, J. E. et al. TRAF2 regulates peripheral CD8(+) T-cell and NKT-cell homeostasis by modulating sensitivity to IL-15. *Eur. J. Immunol.* **45**, 1820–1831 (2015).
16. Yang, X. D. & Sun, S. C. Targeting signaling factors for degradation, an emerging mechanism for TRAF functions. *Immunol. Rev.* **266**, 56–71 (2015).
17. Sun, S. C. The noncanonical NF-kappaB pathway. *Immunol. Rev.* **246**, 125–140 (2012).
18. Li, Y. et al. Cell intrinsic role of NF-kappaB-inducing kinase in regulating T cell-mediated immune and autoimmune responses. *Sci. Rep.* **6**, 22115 (2016).
19. Beinke, S. et al. NF-kappaB1 p105 negatively regulates TPL-2 MEK kinase activity. *Mol. Cell Biol.* **23**, 4739–4752 (2003).
20. Waterfield, M. R., Zhang, M., Norman, L. P. & Sun, S. C. NF-kappaB1/p105 regulates lipopolysaccharide-stimulated MAP kinase signaling by governing the stability and function of the Tpl2 kinase. *Mol. Cell* **11**, 685–694 (2003).
21. Gantke, T., Sriskantharajah, S. & Ley, S. C. Regulation and function of TPL-2, an IkappaB kinase-regulated MAP kinase kinase kinase. *Cell Res.* **21**, 131–145 (2011).
22. Beinke, S., Robinson, M. J., Hugunin, M. & Ley, S. C. Lipopolysaccharide activation of the TPL-2/MEK/extracellular signal-regulated kinase mitogen-activated protein kinase cascade is regulated by IkappaB kinase-induced proteolysis of NF-kappaB1 p105. *Mol. Cell Biol.* **24**, 9658–9667 (2004).
23. Waterfield, M., Jin, W., Reiley, W., Zhang, M. & Sun, S. C. IkappaB kinase is an essential component of the Tpl2 signaling pathway. *Mol. Cell Biol.* **24**, 6040–6048 (2004).
24. Haluszczak, C. et al. The antigen-specific CD8+ T cell repertoire in unimmunized mice includes memory phenotype cells bearing markers of homeostatic expansion. *J. Exp. Med.* **206**, 435–448 (2009).
25. Hogquist, K. A. et al. T cell receptor antagonist peptides induce positive selection. *Cell* **76**, 17–27 (1994).
26. Foulds, K. E. et al. Cutting edge: CD4 and CD8 T cells are intrinsically different in their proliferative responses. *J. Immunol.* **168**, 1528–1532 (2002).
27. Khan, S. H. & Badovinac, V. P. Listeria monocytogenes: a model pathogen to study antigen-specific memory CD8 T cell responses. *Semin. Immunopathol.* **37**, 301–310 (2015).
28. Qiu, Z., Khairallah, C. & Sheridan, B. S. Listeria Monocytogenes: a model pathogen continues to refine our knowledge of the CD8 T cell response. *Pathogens* **7**, 55 (2018).
29. Masopust, D., Kaech, S. M., Wherry, E. J. & Ahmed, R. The role of programming in memory T-cell development. *Curr. Opin. Immunol.* **16**, 217–225 (2004).
30. Kaech, S. M., Hemby, S., Kersh, E. & Ahmed, R. Molecular and functional profiling of memory CD8 T cell differentiation. *Cell* **111**, 837–851 (2002).
31. Porter, B. B. & Harty, J. T. The onset of CD8+-T-cell contraction is influenced by the peak of Listeria monocytogenes infection and antigen display. *Infect. Immun.* **74**, 1528–1536 (2006).
32. Tan, Y. et al. Systemic C3 modulates CD8+ T cell contraction after Listeria monocytogenes infection. *J. Immunol.* **193**, 3426–3435 (2014).
33. Czabotar, P. E., Lessene, G., Strasser, A. & Adams, J. M. Control of apoptosis by the BCL-2 protein family: implications for physiology and therapy. *Nat. Rev. Mol. Cell Biol.* **15**, 49–63 (2014).
34. Yang, K., Neale, G., Green, D. R., He, W. & Chi, H. The tumor suppressor Tsc1 enforces quiescence of naive T cells to promote immune homeostasis and function. *Nat. Immunol.* **12**, 888–897 (2011).
35. D'Souza, W. N., Chang, C. F., Fischer, A. M., Li, M. & Hedrick, S. M. The Erk2 MAPK regulates CD8 T cell proliferation and survival. *J. Immunol.* **181**, 7617–7629 (2008).
36. Srinivasan, L. et al. PI3 kinase signals BCR-dependent mature B cell survival. *Cell* **139**, 573–586 (2009).
37. Kortum, R. L., Rouquette-Jazdanian, A. K. & Samelson, L. E. Ras and extracellular signal-regulated kinase signaling in thymocytes and T cells. *Trends Immunol.* **34**, 259–268 (2013).
38. Tsukamoto, H., Irie, A. & Nishimura, Y. B-Raf contributes to sustained extracellular signal-regulated kinase activation associated with Interleukin-2 production stimulated through the T cell receptor. *J. Biol. Chem.* **279**, 48457–48465 (2004).
39. Watford, W. T. et al. Tpl2 kinase regulates T cell interferon-gamma production and host resistance to Toxoplasma gondii. *J. Exp. Med.* **205**, 2803–2812 (2008).
40. Sun, S. C. Non-canonical NF-kappaB signaling pathway. *Cell Res.* **21**, 71–85 (2011).
41. Sabbagh, L., Pulle, G., Liu, Y., Tsitsikov, E. N. & Watts, T. H. ERK-dependent Bim modulation downstream of the 4-1BB-TRAF1 signaling axis is a critical mediator of CD8 T cell survival in vivo. *J. Immunol.* **180**, 8093–8101 (2008).
42. Wortzman, M. E., Clouthier, D. L., McPherson, A. J., Lin, G. H. & Watts, T. H. The contextual role of TNFR family members in CD8(+) T-cell control of viral infections. *Immunol. Rev.* **255**, 125–148 (2013).
43. Sun, S. C. The non-canonical NF-kappaB pathway in immunity and inflammation. *Nat. Rev. Immunol.* **17**, 545–558 (2017).
44. Tucker, E. et al. A novel mutation in the Nfkb2 gene generates an NF-kappa B2 "super repressor". *J. Immunol.* **179**, 7514–7522 (2007).
45. Croft, M. The role of TNF superfamily members in T-cell function and diseases. *Nat. Rev. Immunol.* **9**, 271–285 (2009).
46. Gardam, S., Sierro, F., Basten, A., Mackay, F. & Brink, R. TRAF2 and TRAF3 signal adapters act cooperatively to control the maturation and survival signals delivered to B cells by the BAFF receptor. *Immunity* **28**, 391–401 (2008).
47. Bouillet, P. et al. Proapoptotic Bcl-2 relative Bim required for certain apoptotic responses, leukocyte homeostasis, and to preclude autoimmunity. *Science* **286**, 1735–1738 (1999).
48. Brightbill, H. D. et al. Conditional deletion of NF-kappaB-Inducing Kinase (NIK) in adult mice disrupts mature B cell survival and activation. *J. Immunol.* **195**, 953–964 (2015).
49. Pearce, E. L. & Shen, H. Generation of CD8 T cell memory is regulated by IL-12. *J. Immunol.* **179**, 2074–2081 (2007).
50. Zou, Q. et al. T cell development involves TRAF3IP3-mediated ERK signaling in the Golgi. *J. Exp. Med* **212**, 1323–1336 (2015).
51. Xiao, G., Harhaj, E. W. & Sun, S. C. NF-kappaB-inducing kinase regulates the processing of NF-kappaB2 p100. *Mol. Cell.* **7**, 401–409 (2001).